MIT Joint Program on the Science and Policy of Global Change

A Three-Dimensional Ocean-Seaice-Carbon Cycle Model and its Coupling to a Two-Dimensional Atmospheric Model: *Uses in Climate Change Studies*

Stephanie Dutkiewicz, Andrei Sokolov, Jeff Scott and Peter Stone

Report No. 122

May* [revised *November*] *2005

The MIT Joint Program on the Science and Policy of Global Change is an organization for research, independent policy analysis, and public education in global environmental change. It seeks to provide leadership in understanding scientific, economic, and ecological aspects of this difficult issue, and combining them into policy assessments that serve the needs of ongoing national and international discussions. To this end, the Program brings together an interdisciplinary group from two established research centers at MIT: the Center for Global Change Science (CGCS) and the Center for Energy and Environmental Policy Research (CEEPR). These two centers bridge many key areas of the needed intellectual work, and additional essential areas are covered by other MIT departments, by collaboration with the Ecosystems Center of the Marine Biology Laboratory (MBL) at Woods Hole, and by short- and long-term visitors to the Program. The Program involves sponsorship and active participation by industry, government, and non-profit organizations.

To inform processes of policy development and implementation, climate change research needs to focus on improving the prediction of those variables that are most relevant to economic, social, and environmental effects. In turn, the greenhouse gas and atmospheric aerosol assumptions underlying climate analysis need to be related to the economic, technological, and political forces that drive emissions, and to the results of international agreements and mitigation. Further, assessments of possible societal and ecosystem impacts, and analysis of mitigation strategies, need to be based on realistic evaluation of the uncertainties of climate science.

This report is one of a series intended to communicate research results and improve public understanding of climate issues, thereby contributing to informed debate about the climate issue, the uncertainties, and the economic and social implications of policy alternatives. Titles in the Report Series to date are listed on the inside back cover.

Henry D. Jacoby and Ronald G. Prinn,
Program Co-Directors

For more information, please contact the Joint Program Office

Postal Address: Joint Program on the Science and Policy of Global Change
77 Massachusetts Avenue
MIT E40-428
Cambridge MA 02139-4307 (USA)

Location: One Amherst Street, Cambridge
Building E40, Room 428
Massachusetts Institute of Technology

Access: Phone: (617) 253-7492
Fax: (617) 253-9845
E-mail: globalchange@mit.edu
Web site: http://MIT.EDU/globalchange/

Printed on recycled paper

A Three-Dimensional Ocean-Seaice-Carbon Cycle Model and its Coupling to a Two-Dimensional Atmospheric Model: Uses in Climate Change Studies

Stephanie Dutkiewicz [1], Andrei Sokolov [2], Jeff Scott [3], and Peter Stone [4]

Abstract

We describe the coupling of a three-dimensional ocean circulation model, with explicit thermodynamic seaice and ocean carbon cycle representations, to a two-dimensional atmospheric/land model. This coupled system has been developed as an efficient and flexible tool with which to investigate future climate change scenarios. The setup is sufficiently fast for large ensemble simulations that address uncertainties in future climate modelling. However, the ocean component is detailed enough to provide a tool for looking at the mechanisms and feedbacks that are essential for understanding the future changes in the ocean system.

Here we show results from a single example simulation: a spin-up to pre-industrial steady state, changes to ocean physical and biogeochemical states for the 20th century (where changes in greenhouse gases and aerosol concentrations are taken from observations) and predictions of further changes for the 21st century in response to increased greenhouse gas and aerosol emissions. We plan, in future studies to use this model to investigate processes important to the heat uptake of the oceans, changes to the ocean circulation and mechanisms of carbon uptake and how these will change in future climate scenarios.

Contents

[1]Department of Earth, Atmospheric and Planetary Sciences, MIT, 54-1412, 77 Massachusetts Ave Cambridge, MA 02139; stephd@ocean.mit.edu

[2]Joint Program for the Science and Policy of Climate Change, MIT; sokolov@MIT.EDU

[3]Department of Earth, Atmospheric and Planetary Sciences, MIT; jscott@wind.mit.edu

[4]Department of Earth, Atmospheric and Planetary Sciences, MIT; phstone@MIT.EDU

1 INTRODUCTION

What will happen to the future climate of our world? Man-induced increases in greenhouses gases (the most important of which is carbon dioxide) is leading to changes in the amount of sun energy that is trapped in the earth system and therefore to changes in the earth's climate itself. Predictions of these changes are hard as the various inter-related mechanisms of heat storage, carbon storage, cloud processes, effects of additional pollutants and the feedback between the different components are not well known and are not easily modelled.

Large three-dimensional earth system models, including representations of the atmosphere, land and ocean processes, are attempting to model future changes. These models are extremely computationally expensive to run, and even with tremendous computer resources still have to parameterize key processes that occur on scales smaller than the models can resolve. Such parameterizations lead to large uncertainties in model-based future predictions of climate change. Moreover, because of the computational cost, such models are fairly inflexible in studying the implications of these uncertainties.

In the late 1990s the Joint Program for the Science and Policy of Global Change at MIT established the "Integrated Global System Model" (hereafter referred to as IGSM1) to examine various aspects of climate change (Prinn *et al.*, 1999). This model included both representations of the climate system (land-atmosphere-ocean) as well as emissions predictions. Unlike the expensive 3-D climate models, this model system included an efficient climate model of intermediate complexity (Sokolov and Stone, 1998) with a 2-D representation of the atmosphere and the ocean. Because of this efficiency, the IGSM1 has been able to be used for ensemble simulations where some of the least well modelled parameters (e.g. cloud feedbacks, ocean heat uptake, future predictions of emissions) could be varied and estimates of the model uncertainties (e.g. Forest *et al.*, 2002) and future change uncertainties (e.g. Webster *et al.*, 2003) could be established.

However, this model in its 2-D setup, is unable to capture the modulation of the ocean circulation in climate change scenarios, and how these circulation changes would affect ocean heat and carbon uptake. The consequences of these missing aspects become particularly

problematic for longer simulations (i.e. simulations past 2100). In order to examine these aspects it is essential to have a 3-D ocean circulation model. Several recent studies (e.g. Kamenkovich *et al.*, 2002; Huang *et al.*, 2003; Dalan *et al.*, 2005) have used 3-D ocean models coupled to the 2-D atmospheric component of the IGSM1 to consider the heat uptake problem. Although these studies have elucidated aspects of the ocean heat uptake, they have not included either interactive seaice or any representation of the carbon cycle.

A new "Integrated Global System Model" (IGSM2) has recently been developed (Sokolov *et al.*, 2005). There have been many improvements to the old model – higher horizontal and vertical resolution in the 2-D atmospheric model, changes to the Emissions Prediction and Policy Analysis (EPPA) model, to the terrestrial component (CLM/TEM/NEM), and the inclusion of the 3-D ocean model with explicit seaice and ocean carbon cycle. This ocean component is discussed in detail in this report.

While the individual ocean/seaice/carbon cycle model components are not new, their coupling together is unique. Here we first discuss each component (Section 2), then describe the techniques used to couple the components to each other and specifically to the 2-D atmospheric component of the IGSM2 (Section 3). This setup (2-D atmosphere/3-D ocean) is still flexible and efficient and will be used in various studies of uncertainty and in atmospheric CO_2 stabilization scenarios, as well as mechanistic studies of heat and carbon uptake. Our goal in this report is to provide detailed information of the ocean-seaice-carbon cycle components and their coupling for future reference. As an illustration of the coupled setup, we will show detailed results of the ocean-seaice-carbon components from a full spin-up to pre-industrial steady-state, 20th century modulations, and 21st century climate change in response to "business-as-usual" emissions predictions (Section 4).

2 MODEL COMPONENTS

In this section we provide brief descriptions and references for the atmospheric/land/economic model components of the IGSM2 and the new 3-D ocean model. We provide a more complete overview of the seaice and carbon models as these are not described in detail, as implemented here, elsewhere in the literature.

2.1 The IGSM2 Atmosphere/Terrestrial/Economic Components

2.1.1 Zonally Averaged Atmosphere

The atmospheric model has been developed from the GISS GCM Model II (Hansen *et al.*, 1983) and has been used extensively for climate change studies (e.g. Sokolov and Stone, 1998; Sokolov *et al.*, 2003). The model solves zonally averaged primitive equations. In this coupled model setup there are 11 vertical layers. In the horizontal there are 4^o zonal bands, except near the poles where there is 2^o resolution. A representation of the land-ocean surface boundary condition horizontal grid for the example simulation described in Section 4 is shown in Figure 1(a).

Each zonal band can consist of land, land ice, ocean and seaice. Surface temperature, turbulent and radiative fluxes and their derivatives are calculated over each type of surface.

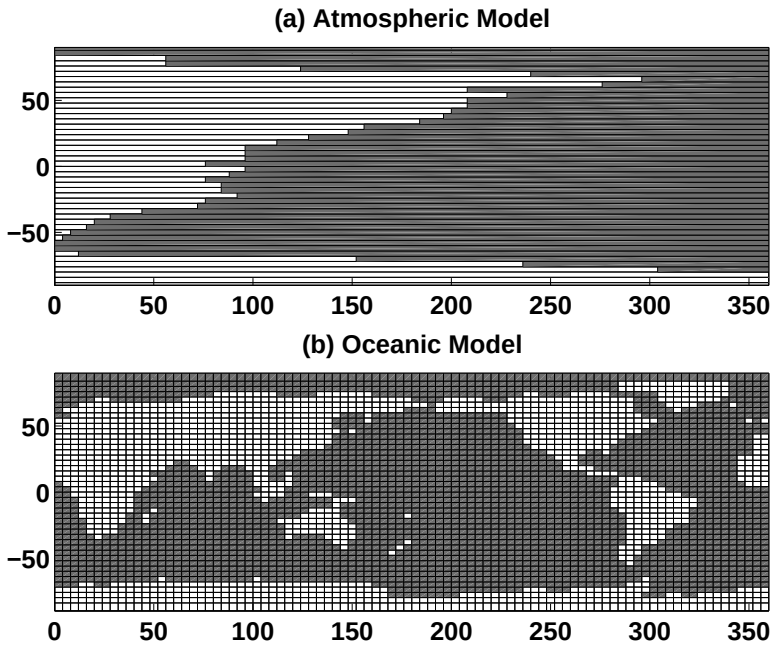

Figure 1: *(a) Representation of atmospheric grid with land/ocean distribution; (b) ocean model grid with land/ocean distribution for the example simulation discussed in Section 4. White regions indicate land in both figures. Atmosphere zonal bands can be further sub-divided into open ocean and seaice, and ice-free land and land ice.*

While calculating flux derivatives, we take into account that surface air temperatures adjust to changes in fluxes (see Kamenkovich *et al.*, 2002 for more details). The main physical processes in the atmosphere are parameterized, as well as the transport of heat, moisture and momentum by eddies. There are complete moisture and momentum cycles which reproduces most of the non-linear interactions and feedbacks simulated by 3-D atmospheric general circulation models. The radiation code includes several greenhouse gases (CO_2, CH_4, N_2O) and several types of aerosols (SO_2, black carbon). More details can be found in Sokolov and Stone (1998).

The above physical model is a key component of the climate model, and is used in all parts of the simulations. In simulations where greenhouse gases and aerosol concentrations are predicted (rather than provided by other data sources), there is also an atmospheric chemistry component (Wang *et al.*, 1998; Wang and Prinn, 1999) that considers the chemical fate of various greenhouse gases and aerosols (e.g. CO_2, NH_4, N_2O, SO_2, black carbon).

2.1.2 Terrestrial and Economic Model Components

The terrestrial hydrography can be provided by a simple, computationally efficient, "bucket" model (Sokolov and Stone, 1998). The IGSM2, though, also has a much more sophisticated terrestrial model which addresses both the surface-heat fluxes and hydrological processes: the Community Land Model (CLM, Bonan *et al.*, 2002) which is based upon the Common Land Model (Zeng *et al.*, 2002) that was derived from a multi-institutional collaboration of land models, and carefully tested (Dai *et al.*, 2003).

In climate prediction simulations, it is also important to consider the storage and emissions of greenhouse gases by the the terrestrial system. In prediction mode, CLM is dynamically linked to the Terrestrial Ecosystems Model (TEM) of the Marine Biological Laboratory (Melillo *et al.*, 1993; Xiao *et al.*, 1997; Zhaung *et al.*, 2004) which simulates the carbon dynamics of terrestrial ecosystems. Further, methane and nitrogen exchange are considered through the Natural Emissions Model (NEM, Liu, 1996), which is driven by dynamic inputs from both TEM and CLM. This version also incorporates the influence of ozone on plant productivity (Feltzer *et al.*, 2004) and the influence of soil thermal regimes on terrestrial carbon and nitrogen dynamics (Zhaung *et al.*, 2003). The coupled CLM/TEM/NEM model system represents the geographical distribution of global land cover and plant diversity through a mosaic approach, in which all major land cover types and plant functional types are considered over given domain (i.e. model grid box), and are area-weighted to obtain aggregate fluxes and storages.

For simulations into the future, the IGSM2 uses the Emissions Prediction and Policy Analysis (EPPA) model to predict emissions of greenhouse gases from nations around the world through estimations of population and economic growth. EPPA is a recursive-dynamical 16-region equilibrium model of the world economy, built on the GTAP dataset (which is maintained by Purdue University). The version used in IGSM2 is updated from Babiker *et al.* (2001)(see Sokolov *et al.*, 2005 for more details).

2.2 The New 3-D Ocean-Seaice-Carbon Model

2.2.1 Ocean

The ocean model is based on the MIT ocean general circulation model (Marshall *et al.*, 1997a,b; http://mitgcm.org/sealion/home_page/frontpage.html). This finite difference model solves the primitive equations for momentum and the advection and diffusion of temperature and salt. The model makes hydrostatic and Boussinesq assumptions.

The horizontal and vertical resolution of the ocean model is flexible. In the example simulation discussed in Section 4, we use a latitudinal resolution of 4^o, except at the poles, where there is 6^o latitudinal resolution (see Fig. 1). In that simulation, the longitudinal resolution is 4^o and there are 15 vertical depth levels: 50m at the surface and increasing to 600m at the bottom.

Since the model is run on a spherical grid, the zonal resolution becomes very small near the poles. Such small grid cells require either very small time-steps (which make the model computationally very expensive) or the use of a filter to reduce the tendency changes. In the example simulation discussed in Section 4, a Fast Fourier Transform (FFT) filter is used in momentum, temperature and salt poleward of 82^o.

The ocean bathymetry can be simple geometry (e.g. rectangular basins as was used in Kamenkovich *et al.*, 2002), or more realistic as used in the example simulation (Section 4). That bathymetry is shown in Figure 2, and is crudely realistic, except for an idealized arctic basin (necessary for the FFT filter).

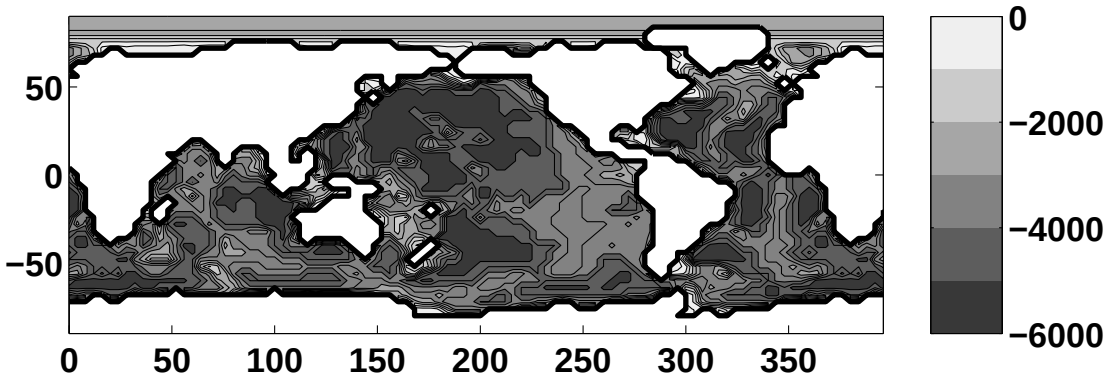

Figure 2: *Ocean model bathymetry (m) used in the example simulation discussed in Section 4. Contour interval is 500m.*

The coarse horizontal resolution means that we do not explicitly capture the mixing induced by eddy motions. A GM mixing scheme (Gent and McWilliams, 1990) can be implemented to parameterize the effect of mesoscale eddies mixing that are not explicitly resolved. In the example simulation in Section 4, the isopycnal diffusivity and isopycnal thickness diffusivity coefficients are both 1×10^3 m^2 s^{-1}, with tapering occurring using the Gerdes *et al.* (1991) method with maximum slope of 0.01.

For numerical stability, as well as to parameterize mixing that occurs across isopycnals,

the model has a implicit diffusion of salt and temperature in the vertical. In the example simulation in Section 4, we use a vertical diffusion of 4×10^{-5} m^2 s^{-1}. In that run the diffusion is increased ten-times in the two layers nearest the bottom (below 1000m) to represent the increased mixing found near the bottom of the ocean. In that run we also use mixing coefficients of 5×10^5 and 1×10^{-3} m^2 s^{-1} for horizontal and vertical viscosity.

In the example simulation (Section 4), we use a simple diffusive convective adjustment procedure implicitly when static instabilities occur. In that run there is no explicit parameterization of mixed layer dynamics, however the ocean model does have the provision for using the K-profile parameterization (KPP) scheme of Large *et al.* (1994).

The time-step is chosen to meet numerical requirements. In the case of the example simulation (Section 4), the time-stepping is asynchronous, with momentum time-step of 900s and a tracer time-step of 12 hours. The advection scheme for salt and temperature is center-difference. In that run there are no-slip conditions for horizontal velocities at lateral walls, and free-slip conditions are used at the bottom. Additionally that run has a linear free surface.

2.2.2 Seaice

Embedded in the ocean model is a thermodynamic seaice model based on the 3-layer model of Winton (2000) and the energy-conserving LANL CICE model (Bitz and Lipscombe, 1999). The model considers two equally thick ice layers; the upper layer has a variable specific heat resulting from brine pockets, the lower layer has a fixed heat capacity. A zero heat capacity snow layer lies above the ice. The ice model is purely thermodynamics – there is no parameterization of ice dynamics. Parameter symbols used (and the values used in the example simulation) are given in Table 1.

Initial Ice Forming: Initial ice forms when open ocean water temperature drops below freezing, $T_f = \mu S_o$, where μ is the ratio of freezing temperature to salinity of brine and S_o is sea surface salinity. The freezing potential of the ocean model surface layer of water is:

$$P_{frz} = (T_f - T_o)(c_{sw}\rho_{sw}\Delta z)$$

where T_o is ocean surface temperature, c_{sw} is seawater heat capacity, ρ_{sw} is the seawater density, Δz is the ocean model upper layer thickness. In order to keep track of the energy in the ice model, we calculate the enthalpy of the ice layers. Enthalpy is defined here as the energy required to melt a unit mass of seaice (and depends on its temperature). For any new ice formed, the enthalpy of the two layers (the upper layer with brine pockets and the lower fresh layer) is calculated as:

$$\begin{aligned} q_1 &= -c_f T_{mlt} + c_i(T_{mlt} - T_f) + L_i(1 - \frac{T_{mlt}}{T_f}) \\ q_2 &= -c_i T_f + L_i \end{aligned}$$

where c_f is specific heat of fresh water, c_i is the specific heat of fresh ice, L_i is latent heat of freezing, ρ_i is density of ice and T_{mlt} is melting temperature of ice with salinity of 1. The

parameter	symbol	value	units
ratio of freezing temperature to salinity of brine	μ	0.054	K/ppt
specific heat of fresh water	c_f	3994	J/kg/K
specific heat of fresh ice	c_i	2106	J/kg/K
density of ice	ρ_i	900	kg/m^3
density of snow	ρ_s	330	kg/m^3
density of fresh water	ρ_f	1000	kg/m^3
density of seawater	ρ_{sw}	1026	kg/m^3
latent heat of freezing	L_i	3.34×10^5	J/kg
thermal conductivity of seaice	K_i	2.03	W/m/K
thermal conductivity of snow	K_s	0.3	W/m/K
heat transfer coefficient	γ	0.006	
ice salinity	S_i	4	psu
reference salinity	S_*	35	psu
minimum ice thickness	$h_{i_{min}}$	0.2	m
maximum ice thickness	$h_{i_{max}}$	5.	m
maximum snow thickness	$h_{s_{max}}$	1.	m
minimum ice fraction	$i_{f_{min}}$	0.1	
maximum ice fration	$i_{f_{max}}$	1.	
height where all freezing occurs over open water	h_{frac}	2.5	m
fraction energy to melting height or extent	f_{extent}	0.4	

Table 1: *Seaice model parameter symbols and the values used in the example simulation (Section 4).*

height of a new layer of ice, determined from the freezing potential and the ice enthalpies, is:

$$h_{i_{new}} = \frac{P_{frz}}{\rho_i q_{av}}$$

where $q_{av} = -\frac{1}{2}(q_1 + q_2)$. The surface skin temperature T_s and ice temperatures T_1, T_2 and the sea surface temperature (T_o) are all set to T_f when new ice is formed.

An ocean grid cell does not need to be either open water or seaice. Fractional ice is implemented by allowing only a portion of the ocean grid cell to freeze. This is done by having a minimum ice thickness, $h_{i_{min}}$, so that the fraction of the cell cover in ice is $h_{i_{new}}/h_{i_{min}}$. There is a minimum ice fraction, $i_{f_{min}}$, and a maximum ice fraction, $i_{f_{max}}$. When a cell already has ice in it, new ice that forms must have ice thickness the same as the ice already in that cell:

$$i_f = (1 - \hat{i_f})\frac{h_{i_{new}}}{h_i}$$

where $\hat{i_f}$ is ice fraction from previous time-step and h_i is current ice height. Snow is redistributed over the new ice fraction.

Growth/Melting of Ice: After initial forming, ice can grow or melt, and have snow deposited on top of it. Heat fluxes at the top and bottom surfaces are used to calculate the change in ice and snow layer thickness.

This model follows the procedure of Winton (2000) (see equations 3 to 21 of that paper) to calculate the surface (T_s) and internal ice temperatures (T_1, T_2). The surface temperature is found from the balance of the flux at the surface Q_s, the shortwave heat flux absorbed by the ice, and the upward conduction of heat through the snow and/or ice, Q_u. Q_s is linearized about the surface temperature as:

$$Q_s(T_s) = Q_s(\hat{T_s}) + \frac{\partial Q_s(\hat{T_s})}{\partial T_s}(T_s - \hat{T_s})$$

where $Q_s(\hat{T_s})$ and $\frac{\partial Q_s(\hat{T_s})}{\partial T_s}$ are the surface heat flux and its derivative with regard to surface temperature at the previous time-step, $\hat{T_s}$. These are provided by the atmospheric model. The conductive flux to the surface is:

$$Q_u = K_{1/2}(T_1 - T_s)$$

where $K_{1/2}$ is the effective conductive coupling of the snow-ice layer between the surface and the mid-point of the upper layer of ice $K_{1/2} = \frac{4K_iK_s}{K_sh_i+4K_ih_s}$. K_i and K_s are constant thermal conductivities of seaice and snow.

New temperatures are calculated at each time-step. The surface temperature is not allowed to be greater than zero. The new enthalpies of the seaice layers are calculated based on their new temperatures:

$$\begin{aligned} q_1 &= -c_f T_f + c_i(T_f - T_1) + L_i(1 - \frac{T_f}{T_1}) \\ q_2 &= -c_i T_2 + L_i. \end{aligned}$$

The energy flux at the surface available for melting (if T_s=0) and the energy at the ocean-ice interface for either melting or freezing are calculated from the new ice temperatures:

$$\begin{aligned} E_{top} &= (Q_s - K_{1/2}(T_s - T_1))\Delta t \\ E_{bot} &= (\frac{4K_i(T_2 - T_f)}{h_i} - Q_b)\Delta t \end{aligned}$$

where Q_b is the heat flux at the ice bottom due to the sea surface temperature variations from freezing, and Δt is the time-step. If T_o is above freezing, $Q_b = c_{sw}\rho_{sw}\gamma(T_o - T_f)u^*$, γ is the heat transfer coefficient and u^* is frictional velocity between ice and water. If T_o is below freezing, $Q_b = (T_f - T_o)c_f\rho_f\Delta z/\Delta t$ (where ρ_f is density of fresh water). After Q_b is calculated, the ocean temperature is set to T_f.

If $E_{top} > 0$, snow melts from the surface, if all the snow is melted and there is energy left, ice melts. If the ice is all gone and there is still energy left, this energy is applied to heating the ocean model upper layer (see Winton, 2000 equations 27-29). Similarly if $E_{bot} > 0$, ice melts from the bottom. If all the ice is melted, the snow is melted (with energy from the ocean model upper layer if necessary). If $E_{bot} < 0$, ice grows at the bottom as:

$$\Delta h_i = \frac{-E_{bot}}{(q_{bot}\rho_i)}$$

where $q_{bot} = -c_i T_f + L_i$ is the enthalpy of the new ice. The enthalpy of the second ice layer, q_2 needs to be modified:

$$q_2 = \frac{\hat{h_i}/2\hat{q_2} + \Delta h_i q_{bot}}{\hat{h_i}/2 + \Delta h_i}$$

If there is an ice layer and the overlying air temperature is below 0^oC then any precipitation, P joins the snow layer:

$$\Delta h_s = -P\frac{\rho_f}{\rho_s}\Delta t,$$

ρ_f and ρ_s are the fresh water and snow densities. Any evaporation, similarly, removes snow or ice from the surface.

For practical reasons there is a maximum ice height, $h_{i_{max}}$, and maximum snow height, $h_{s_{max}}$. Ice and/or snow above these limits are converted back to water, maintaining the salt balance. Note however, that heat is not conserved in this conversion; sea surface temperatures below the ice are not recalculated. If the snow/ice interface is below the waterline, snow is converted to ice (see Winton, 2000, equations 35 and 36). Ice is repartitioned into equal thickness layers while conserving energy.

Heat and fresh water fluxes from the seaice model affect the ocean model surface layer temperature and salinity. The heat flux:

$$q_{net} = q_{sw} - Q_b - \frac{E_{surp}}{\Delta t} \tag{1}$$

is composed of the shortwave flux that has passed through the ice layer, q_{sw} and is absorbed by the water, the ocean flux to the ice Q_b, and the surplus energy left over from the melting,

E_{surp}. The fresh water flux is determined from the amount of fresh water and salt in the ice/snow system before and after the time-step (excluding any newly accumulated snow):

$$f_{net} = \frac{\rho_s(h_s - \hat{h_s}) + \rho_i(h_i - \hat{h_i})}{\Delta t} - P|_{T_a=0} - \frac{\rho_i S_i(h_i - \hat{h_i})}{S_* \Delta t} \tag{2}$$

where the $\hat{}$ refers to the quantity at the previous time-step. S_i is the ice salinity, and S_* is a reference salinity. From this equation we see that when ice freezes there is a brine rejection which will increase surface ocean salinity, and when ice melts there is a flux of fresh water which decreases the surface ocean salinity.

If ice height is above a certain height, h_{frac}, then all energy from freezing at sea surface is used only in the open water parts of the cell (i.e. Q_b will only have the conduction term). The melt energy is partitioned, f_{extent}, between melting ice height and ice extent. However, once ice height drops below the minimum height, $h_{i_{min}}$, then all energy melts ice extent.

2.2.3 Ocean Carbon

The ocean carbon model considers the movement of total dissolved inorganic carbon (DIC) within the ocean and the exchange of carbon with the atmosphere. Total dissolved carbon is made up of carbon dioxide and carbonic acid ($[CO_2^*] = [CO_2] + [H_2CO_3]$, which are difficult to distinguish analytically) and other carbonate species:

$$DIC = [CO_2^*] + [HCO_3] + [CO_3].$$

The physical ocean model velocity and diffusivities are used to redistribute DIC within the ocean. Additional redistribution of DIC comes from the "biological pump", the fluxing of carbon from surface waters to depth as sinking organic matter. However, since carbon is rarely a limiting nutrient in biological production we must follow the fate of some other limiting macro-nutrient. Here we chose to use phosphorus as the currency of biological productivity in the model. We, therefore, follow 4 biogeochemical tracers in this component of the model: DIC, Alkalinity (ALK), phosphate (PO_4) and dissolved organic phosphorus (DOP). For any of these tracers, A, the prognostic equation of the model is:

$$\frac{\partial A}{\partial t} = -\nabla \cdot (\vec{u^*} A) + \nabla \cdot (\mathbf{K} \nabla A) + S_A$$

where $\vec{u^*}$ is the transformed Eulerian mean circulation (which includes Eulerian and eddy-induced advection), $\mathbf{K}$ is the mixing tensor, and S_A are the sources and sinks due to biological and chemical processes. The ocean model provides the advective and diffusive parts of this equation, and the "SuperBee" second order flux limiter advection scheme (Roe, 1985) is used so as to limit spurious negatives. Here we describe more completely the source/sink terms, S_A (see Table 2 for symbols, parameter values are those used in the example simulation, Section 4):

$$S_{DIC} \;=\; F_{CO_2} + V_{CO_2} + r_{C:P} S_{PO_4} + J_{Ca} \tag{3}$$

$$S_{ALK} = V_{ALK} - r_{N:P} S_{PO_4} + 2J_{Ca} \quad (4)$$

$$S_{PO_4} = -J_{prod} - \frac{\partial F_P}{\partial z} + \kappa_{remin}[DOP] \quad (5)$$

$$S_{DOP} = f_{DOP} J_{prod} - \kappa_{remin}[DOP]. \quad (6)$$

F_{CO_2} is the flux of CO_2 from the ocean to the atmosphere:

$$F_{CO_2} = k_w([CO_2] - [CO_2]_{sat}).$$

where k_w is the gas transfer velocity, $[CO_2]$ is sea surface concentration of carbon dioxide and $[CO_2]_{sat}$ is the partial pressure of CO_2 in the water if it were fully saturated. The gas transfer coefficient is parametrized following Wanninkhof (1992) and is a function of the wind speed (provided by atmospheric model), and Schmidt number (a function of surface sea temperature). Surface ocean $[CO_2]$ is determined from local DIC, alkalinity, temperature, salinity, boron, phosphate and silicon concentrations. Total boron is parameterized as a function of salinity, and total silicon is assumed constant. The remaining variables are carried as tracers in the model. $[CO_2]_{sat}$ is determined as a function of partial pressures of CO_2 in the air, atmospheric pressure, sea surface temperature, and salinity. There is no air-sea flux of CO_2 where there is seaice. All coefficients of the air-sea flux calculations are determined using the algorithms used in the ocean carbon modeling inter-comparison project (OCMIP) (Najjar and Orr, 1998; Matsumoto *et al.*, 2004). More detail can be found in Millero (1995) and DOE Handbook (1994).

Our ocean model does not take into account the changes to tracer concentrations due to the surface freshwater fluxes. Such changes are of negligible importance for most of the tracers, but does impact the CO_2 chemistry sufficiently that we need to take this "virtual flux" into account (see Najjar and Orr, 1998):

$$V_{CO_2} = \frac{\overline{DIC}_s}{\overline{S_o}} \frac{S_* F}{\Delta z},$$

where $\overline{DIC}_s$ and $\overline{S_o}$ are the global surface mean DIC and salinity concentrations, F is the local freshwater flux, $S_* = 35$psu is a reference salinity, and Δz is upper layer thickness.

The remainder of the terms in Eq. 3 are defined by the parameterization of the biological pump. We calculate biological production (the net community productivity) as a function of light, I and nutrient (phosphate, PO_4) availability (similar to McKinley *et al.*, 2004):

$$J_{prod} = \alpha \frac{I}{I + \kappa_I} \frac{PO_4}{PO_4 + \kappa_{PO_4}}$$

where κ_I and κ_{PO_4} are half-saturation values typical of ocean biology. The format of this light and phosphate limitation follows Michaelis-Menten kinetics. The parameter α is the maximum community production rate. Light, here, is that portion of the short wave radiation that is photo-synthetically available, and that has not been attenuated as it travels through the water column:

$$I = f_{PAR} Q_{sw} e^{-kz}.$$

parameter	symbol	value	units
light half saturation	κ_I	25	W/m^2
phosphate half saturation	κ_{PO_4}	5×10^{-4}	mol/m^3
light attenuation	k	0.02	1/m
PAR fraction	f_{PAR}	0.4	
maximum community production	α	3×10^{-3}	$mol/m^3/y$
fraction new production going to DOP	f_{DOP}	0.67	
DOP remineralization rate	κ_{remin}	2	1/y
power law remineralization coefficient	a_{remin}	0.9	
ratio carbon to phosphorus	$r_{C:P}$	117	
ratio nitrogen to phosphorus	$r_{C:P}$	16	
rain ratio	R	0.07	
scale depth for $CaCO_3$ remineralization	d_{Ca}	3500	m

Table 2: *Ocean carbon cycle model parameter symbols and the values used in the example simulation (Section 4).*

Most of the biological production occurs in the upper layers of the ocean model. Q_{sw} is supplied by the atmospheric model.

A portion (almost 70%, Yamanaka and Tajika, 1997) of the biological production ($f_{DOP}J_{prod}$) in the upper layer of the ocean remains suspended in the water column as dissolved organic phosphorus, which remineralizes back to phosphate with a rate κ_{remin}. The remainder of the biological production becomes particulate organic phosphorus (POP) which sinks to depths, and is parameterized as instantly remineralizing to phosphate. The flux decreases with depth due to remineralization following a power law relationship (following OCMIP, Najjar and Orr, 1998):

$$F_p = (1 - f_{DOP})J_{prod}\Delta z(\frac{z}{z_c})^{-a_{remin}}$$

where z_c is depth of base of each layer (with thickness Δz) where production occurs and a_{remin} is chosen to provide remineralization length scales of a few hundred meters (Sarmiento *et al.*, 1990, Yamanaka and Tajika, 1997).

The fate of DIC is tied to that of phosphorus through the Redfield ratio $r_{C:P}$ (see Eq. 3). However carbon is also exported to depth in the calcium carbonate shells that some plankton form. This is accounted for by the final term, J_{Ca}, in Eq. 3. Here we follow the parameterization of Yamanaka and Tajika (1996), where the calcium carbonate formation is proportional to the particulate organic phosphorus produced in the surface waters by the "rain-ratio" (R, the ratio of hard and soft tissue produced). The term for dissolution is:

$$J_{Ca} = -Rr_{C:P}(1 - f_{DOP})J_{prod} + \frac{\partial F_{CaCO3}}{\partial z}$$

also includes the accumulation of the downward flux of $CaCO_3$, F_{CaCO3}, which is assumed to decrease exponentially with a depth scale of d_{Ca}:

$$F_{CaCO3} = Rr_{C:P}(1 - f_{DOP})J_{prod}\Delta z e^{-(z-z_c)/d_{Ca}}.$$

Alkalinity cycling, which is important in determining ocean [CO_2] concentrations, is linked to the phosphate cycle (through ratio of nitrogen to phosphorus, $r_{N:P}$) and through the calcium cycle following Najjar and Orr (1998) (see Eq. 4). The effect of freshwater fluxes on alkalinity concentrations are also taken into account, similar to that of CO_2:

$$V_{ALK} = \frac{\overline{ALK}_s}{\overline{S_o}} \frac{S_* F}{\Delta z},$$

where $\overline{ALK}_s$ is global surface mean alkalinity.

3 COUPLING PROCEDURE

3.1 Model Dialog

Typically the atmospheric model uses a significantly shorter time-step than the ocean model. The standard format used in this coupled system is to pass information between atmosphere and ocean models every 24 hours (although the setup is flexible enough for other timings). As an example, in the simulation discussed in Section 4, the atmospheric model runs for 24 hours using zonally averaged sea surface and ice surface temperatures, the fraction of ocean covered by seaice, and air-sea CO_2 fluxes (Table 3). The atmospheric model, in its turn, supplies the ocean-ice-carbon model with zonal mean heat flux, evaporation, and their derivatives with respect to surface temperature; as well as precipitation, runoff from the land, wind stress, sea-surface atmospheric pressure, incident short-wave radiation and atmospheric CO_2 content (Table 4). In the next few sections we describe several methods by which 2-D fields used to force an ocean model are produced from the atmospheric model outputs.

$\overline{T_o}$	zonally averaged sea surface temperature
$\overline{T_i}$	zonally averaged seaice skin temperature
f_i	fraction of latitude band covered in ice
$\overline{F_{CO_2}}$	zonally averaged air-sea CO_2 flux

Table 3: *Quantities passed from 3-D ocean/seaice/carbon cycle model to 2-D atmsopheric model.*

For completeness, we also include tables with the connections between the ocean module and the seaice module and between the ocean/seaice modules and the ocean carbon cycle module (Table 5). The seaice and carbon models have the same time-step as the salt and temperature tracers in the ocean model. The connections between these components and the atmospheric model are schematically represented in Figure 3.

3.2 Zonal Variations for Atmospheric Fluxes

3.2.1 Heat and Evaporation

Here we use the derivatives of the heat flux and evaporation with respect to surface temperature (provided by the atmospheric model) to produce zonal variations in the fluxes as

for ocean	
Q_o	heat flux to open ocean
E_o	evaporation to open ocean
$\partial Q_o/\partial T$	derivative of heat flux with respect to surface temperature
$\partial E_o/\partial T$	derivative of evaporation with respect to surface temperature
P	precipitation
R	runoff
τ_x	zonal wind stress
τ_y	meridional wind stress
for seaice	
Q_i	heat flux over seaice
E_i	evaporation over seaice
$\partial Q_i/\partial T$	derivative of heat flux with respect to surface temperature
$\partial E_i/\partial T$	derivative of evaporation with respect to surface temperature
P	precipitation
T_a	surface air temperature
Q_{sw}	short-wave radiation
for carbon model	
w_s	wind speed
P_a	atmospheric pressure at sea surface
Q_{sw}	short-wave radiation
pCO_2	atmospheric partial pressure of CO_2

Table 4: *Quantities passed from 2-D atmospheric model to 3-D ocean/seaice/carbon cycle model.*

from ocean to ice	
T_o	local sea surface temperature (SST)
S_o	local sea surface salinity (SSS)
$\vec{V}$	local ocean current velocity
from ice to ocean	
i_f	fraction of grid cell covered in ice
q_{net}	heat flux
f_{net}	freshwater flux
from ocean/seaice to carbon cycle	
T_o	local sea surface temperature
S_o	local sea surface salinity
i_f	fraction of grid cell covered in ice

Table 5: *Quantities passed between 3-D ocean, seaice and carbon cycle models.*

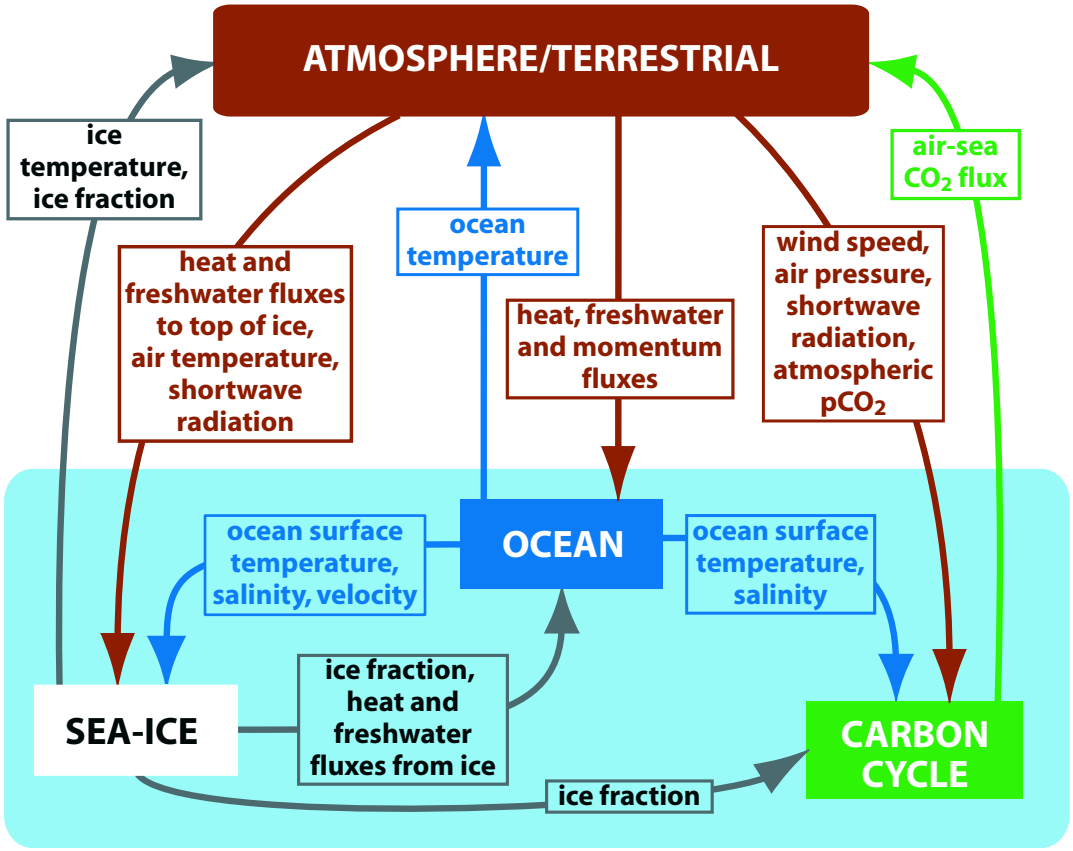

Figure 3: *Schematic of connections between different components of the ocean/seaice/carbon cycle model and their connections to the atmospheric model.*

in Kamenkovich *et al.* (2002):

$$Q(x,y) = Q_z(y) + (\frac{\partial Q}{\partial T})_z(T_s(x,y) - T_z(y)) \quad (7)$$

$$E(x,y) = E_z(y) + (\frac{\partial E}{\partial T})_z(T_s(x,y) - T_z(y)) \quad (8)$$

where subscript z refers to zonal mean values provided by the atmospheric model, and subscript s refers to surface values (either for seaice or open ocean).

3.2.2 Runoff

Zonal integrated runoff calculated by the land model is converted into fresh water flux to the ocean using a weighting function. As an example of the use of this runoff weighting function, we describe the system used in the example simulation of Section 4. In that simulation, we use the river outflow data from Perry *et al.* (1996), adapted to the ocean grid (Figure 4). The IPCC Report (2001) suggests values of runoff and iceberg-production from Greenland of 525×10^{12} kg y^{-1} and from Antarctica of 2246 $\times10^{12}$ kg y^{-1}. These discharges have been distributed about the respective land masses. The values in this figure are donated as the observational runoff $R_{data}(x,y)$. The data is then divided into five zonal bands denoted by the heavy lines in Figure 4. Each grid cell is then give a weighting:

$$W(x,y) = \frac{R_{data}(x,y)}{\sum_{band} R_{data}(x,y)}.$$

Land runoff ($R_z(y)$) in each band is summed ($\sum_{band} R_z(y)$), and this is distributed following the weighting function given above, so that runoff information received by the ocean model is:

$$R(x,y) = W(x,y) \sum_{band} R_z(y). \quad (9)$$

The ocean model therefore has freshwater input at locations where there are significant rivers.

The locations of the bands can be easily moved as necessary. This procedure could be used for different model configurations. The weighting function is also flexible, and a more idealized representation $R_{data}(x,y)$ can be provided.

3.3 Other Modifications to Fluxes

The coupled model setup described this far can be run as an effective climate model. However, often the resulting circulations of atmosphere and ocean are not similar to that of the present day climate. Parameterization problems, resolution problems, problems with conversion from 1-D fields to 2-D forcing fields, and other mismatches in the different components lead to a solution which has drifted far from present day. Models frequently use flux adjustments in order to prevent their simulations from drifting away from the current climate (McAvaney *et al.*, 2001). Since here we are interested in future climate scenarios, it is crucial that we produce a credible present day climate in our model spin-up. We are

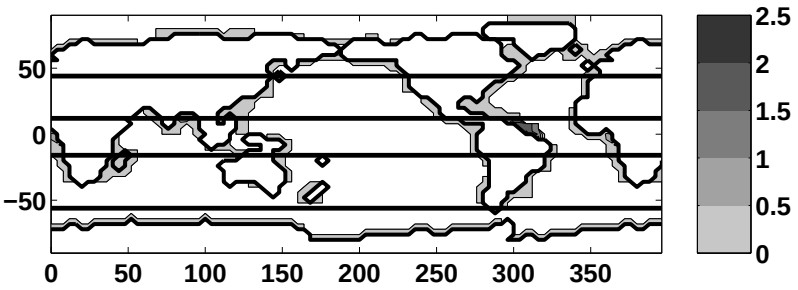

Figure 4: *River runoff (10^4 m^3 s^{-1}) used as part of the weighting function for the conversion from atmospheric to ocean model runoff in the example simulation (Section 4). Data comes from Perry et al. (1996), with smoothing of each river output to the surrounding closest ocean points. Values for ocean points around Greenland and Antarctica ice melt are taken from IPCC Report (2001).*

therefore forced to make some modification to the forcing fields applied to the ocean. For instance for a surface flux, A, the flux to the ocean is:

$$A_o(x, y) = A_{atm} - A_{adj}(x, y).$$

We discuss some of the possible ways to adjust these fluxes next.

3.3.1 Anomaly Coupling

A technique often employed in coupled models (e.g. Voss *et al.*, 1998) is to take the mean present day value of some flux (e.g. wind stress to the ocean) from observations and the anomalies from the atmospheric model. In this anomaly coupling procedure a flux $A_o(x, y)$ provided to the ocean model is deduced from the atmospheric instantaneous value, A_{atm}, with model climatological value, $\overline{A_{atm}}^t$, subtracted out and the observed climatological value, $A_{obs}(x, y)$ added back:

$$A_o(x, y) = A_{atm} - \overline{A_{atm}}^t + A_{obs}(x, y). \tag{10}$$

Atmospheric values may be 2-D fields constructed as described in Section 3.2.1 or zonal means. In the case where A_{atm} is only a zonal mean, this procedure also provides a way for the ocean model to be forced with a 2-D field. In this case $A_{adj} = \overline{A_{atm}}^t - A_{obs}(x, y)$.

3.3.2 Flux Adjustment to Surface Values

Models of both the atmosphere and ocean have inherent flaws, mainly arising from subgridscale parameterizations. Even an ocean circulation model that is forced by the best available observations of atmospheric fluxes, will not provide completely realistic circulations. Similarly, an atmospheric model provided with exact sea surface temperatures (SST) will also drift away from observed behavior. Although these drifts may be small, they lead to problems with the coupled model results over long periods.

Some of these problems can be compensated for by an additional term to the fluxes provided to the ocean, calculated at each time-step to bring the model surface fields back into consistency with observations. In this case the $A_{adj}(x, y)$ is a damped term bringing a surface value back to an observed value. For instance, for heat flux, Q and freshwater fluxes, F these additional terms would be:

$$Q_{adj}(x, y) = \lambda_T(T_o(x, y) - T_{obs}(x, y)) \quad (11)$$
$$F_{adj}(x, y) = \lambda_S(S_o(x, y) - S_{obs}(x, y)). \quad (12)$$

These terms can be thought of as the fluxes necessary to adjust for the shortcomings of the model itself. Using them has the virtue that there are important climate feedbacks that are very sensitive to surface temperatures, e.g., water vapor and ice-albedo feedbacks, and using flux adjustments to obtain realistic temperatures in the current climate ensures that these feedbacks are simulated accurately for modest climate changes (Shackley *et al.*, 1999).

In a study of climate change, however, this procedure becomes a problem – it does not allow for a predictive quality in the coupled system, but constrains the model to present day observations. In this coupled model, we provide the possibility of spinning up with the relaxation term, and then using an average of this term later as a "fixed flux adjustment".

3.3.3 Flux Adjustment to Observed Fluxes

Sometimes it is desirable to run in a spin-up mode with fluxes taken directly from observations. In this procedure the ocean model is spun to steady state with the observed flux (for instance freshwater fluxes, F_{obs}). To allow the model to then be used in predictive capacity for a changing climate, the difference between the atmospheric freshwater forcing and the observations is calculated over some climatological timescale:

$$F_{adj}(x, y) = \overline{(E(x, y) - P(y) - R(x, y))} - F_{obs}(x, y)$$

where E(x,y) comes from Eq. 8, R(x,y) from Eq. 9 and P(y) is precipitation (all provided by the atmospheric model). This term can then be applied as a fixed adjustment to the fluxes in the continuation of the model simulation. This procedure is in essence, but not in implementation, almost identical to anomaly coupling. We do not use this procedure in the example simulation of Section 4, but will use it in some simulations in future studies.

The coupled model described here is quite versatile in the techniques of the coupling. It can be run with no additional modifications to the atmospheric fluxes, or with anomaly coupling and/or flux adjustments and/or observed fluxes. In the next section we discuss one combination of coupling procedure and the results from that "example" simulation.

4 EXAMPLE SIMULATION: PRESENT DAY AND FUTURE CLIMATE

As an example of the coupled system, we provided detailed results from a simulation of the 20th and 21st century. However, it is important to keep in mind that this represents just one set of model parameters, coupling procedures and future emission scenarios. Changing model parameters (e.g. vertical diffusion, viscosities, GM-values, biological community uptake rates) will have differing impacts on the results. The coupling procedure and flux adjustments also will impact the results and behavior of the model to changes. A more comprehensive look over a wide range of parameter choices will provide a better sense of the model uncertainties.

The simulation described in this section is carried out in four phases. Seaice and carbon model parameters are provided in Tables 1 and 2. In all phases the atmosphere model runs for 24 hours; the final values of heat, freshwater, and momentum fluxes are then used to force the ocean model forward for 24 hours (with a time-step of 12 hours). As described in more detail below, the momentum forcing is done through anomaly coupling and heat and freshwater fluxes have adjustments to maintain SST and sea surface salinity (SSS) close to modern observations for spin-up of the late 20th century.

4.1 Simulation Setup

Phase 1: In the first phase the atmospheric model runs with fixed greenhouse gases and forcing for 1980 conditions. We run with only atmosphere physics, ocean, seaice and land hydrology. The ocean carbon cycle is neglected during this phase.

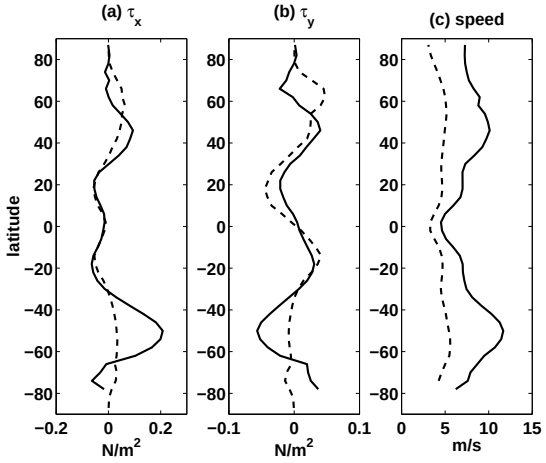

Figure 5: *Annual average (a) zonal wind stress (N m^{-2}); (b) meridional wind stress (N m^{-2}); (c) wind speed (m/s). Solid line is from Trenberth et al. (1989); dashed line is from atmospheric model.*

Figure 5 compares the components of the annual wind stress from the atmospheric model (solid line) to that from Trenberth *et al.* (1989). Although these are reasonably matched

in the tropics, the model strongly underestimates winds in the mid-to-high latitudes, especially in the southern hemisphere. This leads the ocean model to have a very weak Antarctic Circumpolar Current (ACC) – a serious problem as the Southern Ocean circulation is very important in producing water masses that affect the distribution of salt, temperature, and DIC. We employ the technique of "anomaly" coupling for the wind stress and wind speeds in our model. Here we take a 24-hour wind value, subtract out the atmospheric model climatological value for steady state and replace it with the climatological value from observations (Trenberth *et al.*, 1989, Fig. 6). The atmospheric model climatological values are calculated as monthly mean values for 100 years at steady-state. These are then linearly interpolated to the exact time-step. Similarly, the Trenberth *et al.* (1989) climatological monthly values are interpolated to each time-step.

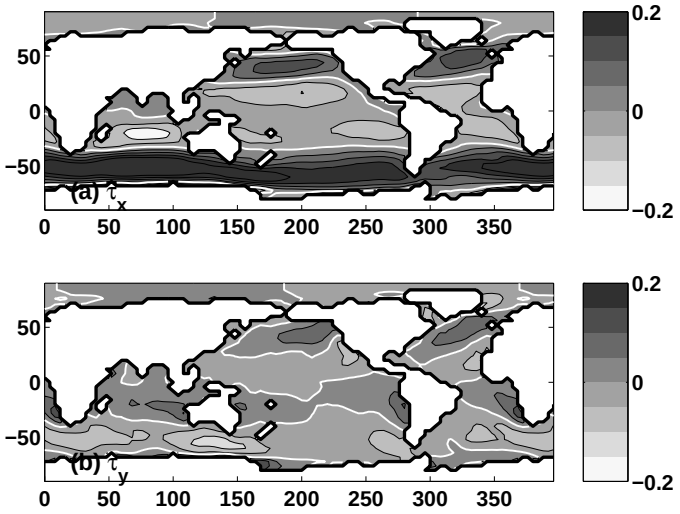

Figure 6: *Annual average climatology of wind stress (N m^{-2}) from Trenberth et al. (1989): (a) zonal, (b) meridional. Zero contour is white, and contour interval is 0.05 N m^{-2}.*

Without any correction, SST and SSS drift from current day values. We therefore find it necessary to adjust the heat and freshwater fluxes. This flux adjustment is done by relaxing SST and SSS toward the monthly climatological means of Levitus and Boyer (1994) and Levitus *et al.* (1994).

We spin the model up for 1500 years with the following forcing over the ocean:

$$\tau_x(x,y) = \tau_{x_z}(y) - \overline{\tau_{x_z}(y)}^t + \tau_{x_{tren}}(x,y) \quad (13)$$

$$\tau_y(x,y) = \tau_{y_z}(y) - \overline{\tau_{y_z}(y)}^t + \tau_{y_{tren}}(x,y) \quad (14)$$

$$Q_T(x,y) = Q_o(x,y) - Q_{adj}(x,y) \quad (15)$$

$$F_T(x,y) = E_o(x,y) - P(y) - R(x,y) - F_{adj}(x,y) \quad (16)$$

where $\overline{\tau_{x_z}(y)}^t$ and $\overline{\tau_{y_z}(y)}^t$ are interpolated from 100 year monthly averages. These are updated every few hundred years of this phase of the spin-up. $Q_o(x,y)$ and $E_o(x,y)$ are as

given in Eq. 7 and Eq. 8 (including meridional variations derived from the derivative with respect to surface temperature), $R(x,y)$ is from Eq. 9. Relaxation terms, $Q_{adj}(x,y)$ and $F_{adj}(x,y)$, are from Eq. 11 and Eq. 12. Since there are problems associated with the relaxation terms $Q_{adj}(x,y)$ and $F_{adj}(x,y)$ near to and under the seaice, we use a relaxation timescale that is latitude dependent. At the equator λ is 30 days, but drops off so that it is zero poleward of 60^o.

The ocean under the ice is provided with fluxes:

$$\begin{aligned} \tau_x(x,y) &= 0 \\ \tau_y(x,y) &= 0 \\ Q_T(x,y) &= q_{net}(x,y) \\ F_T(x,y) &= f_{net}(x,y) - P(y)|_{T_a \neq 0} - R(x,y). \end{aligned}$$

The ocean is not affected by wind forcing under the ice, the heat flux is that found from the ice model, q_{net} (Eq. 1). The freshwater flux is a combination of that from the ice model f_{net} (Eq. 2), from any precipitation (when the air temperature is above 0^oC) and from runoff, $R(x,y)$ from Eq. 9. In grid cells where there is ice and open water, the fluxes passed to the ocean are an average of the fluxes for open ocean and for below ice, weighted by the ice fraction.

The model is started from rest, with initial temperature and salinity fields taken from Levitus and Boyer (1994) and Levitus *et al.* (1994). After 1500 years the model is approaching a steady-state for the forcing of 1980. Figures 7 and 8 show the zonal atmospheric fluxes (a), the addition of the derivative term (Eq. 7 and Eq. 8) and effects of seaice (b), and the final fluxes used by the ocean model, that includes the $Q_{adj}(x,y)$ and $F_{adj}(x,y)$ terms (c).

Flux adjustments are used in many coupled atmosphere-ocean GCMs in order to prevent their simulations from drifting away from the current climate (McAvaney *et al.*, 2001). The procedure can be rigorously justified if the adjustments are small compared to the model generated fluxes (Sausen *et al.*, 1988), but unfortunately they frequently are not (McAvaney *et al.*, 2001). The problem is compounded in a model like ours, where the zonal variations in surface fluxes must be parameterized. In fact the flux adjustments we use are of order one, i.e. the global root mean square (rms) of Q_{adj} is 35 W m^{-2} compared to rms of the total heat flux, 34W m^{-2}, and for the freshwater adjustment, 3.13×10^{-8} compared to 2.92×10^{-8}. Using such flux adjustments is undesirable because it means that heat and moisture are no longer being conserved at the surface. Nevertheless using them has the virtue that there are important climate feedbacks whose strength depends on surface conditions, and which will not be simulated accurately in our model without these flux adjustments.

In this phase the atmosphere (with no chemistry), ocean with seaice (but no carbon cycle) and CLM components are used. On a 3 GHz Pentium 4 chip, each year of model integration takes 10 minutes (3 in atmosphere, 4 in the land hydrography, and 3 in ocean/seaice).

Phase 2: The flux adjustment terms $Q_{adj}(x,y)$ and $F_{adj}(x,y)$ are averaged (monthly) over the last 100 years of phase 1. The second phase of the spin-up then uses these fields (linearly interpolated between months for each time-step), as fixed flux adjustment, and

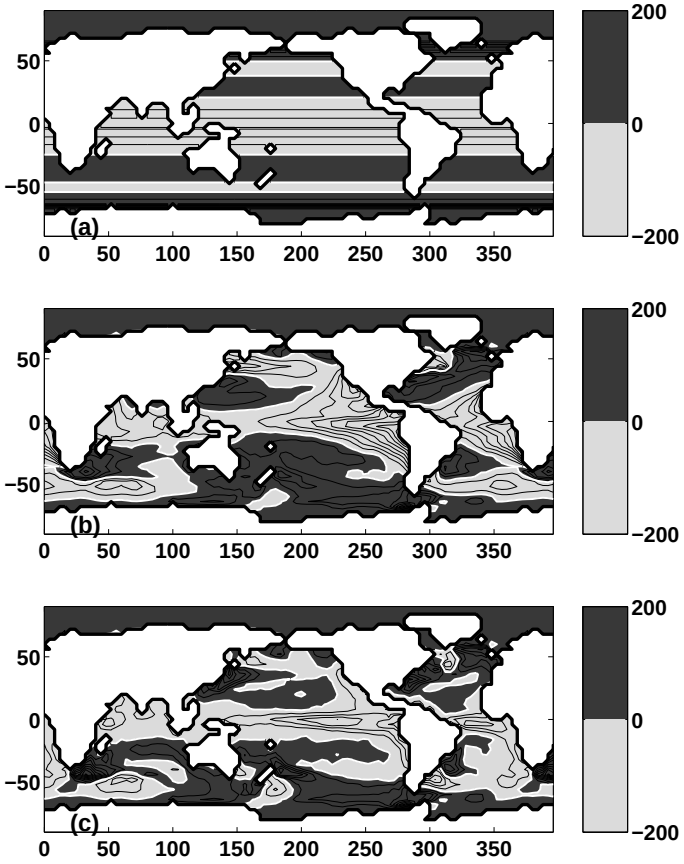

Figure 7: *Heat Flux (W m^{-2}) at end of phase 1: (a) from zonal atmospheric model to open ocean (note here that seaice has not been taken into account); (b) including also zonal variations provided by the atmospheric model derivatives with respect to surface temperature (Eq. 7) and including ice effects (Eq. 1); and (c) with the addition of the term needed to maintain SST near that of observations (Eq. 11). Contour interval is 25 W m^{-2}, and the zero contour is white. Positive values (dark shading) indicate loss of heat from the ocean.*

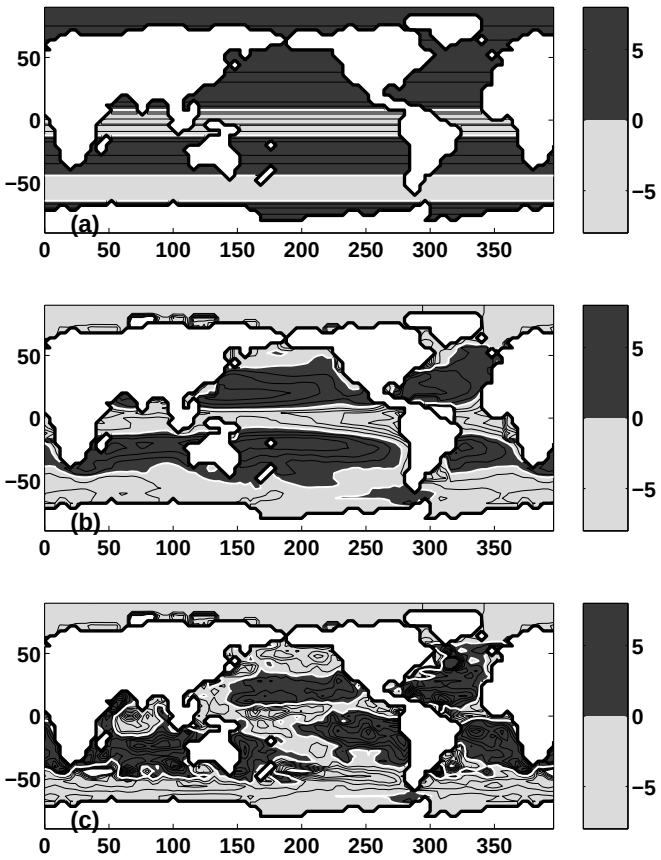

Figure 8: *Freshwater Flux (10^{-8} m s^{-1}) at end of phase 1: (a) from zonal atmospheric model to open ocean; (b) with the addition of the zonal variations provided by the atmospheric model derivatives with respect to surface temperature to the evaporation (Eq. 8), variations of runoff (Eq. 9), and including ice effects (Eq. 2); and (c) with the addition of the term needed to maintain SSS near that of observations (Eq. 12). Contour interval is 1 × 10^{-8} m s^{-1} and the zero contour is white. Positive values (dark shading) indicates a net loss of freshwater.*

there is no more active relaxing to SST and SSS. We also use the final update of $\overline{\tau_{x_z}(y)}^t$ and $\overline{\tau_{y_z}(y)}^t$ in this second phase.

The real ocean state of 1980 and its carbon inventory are not in steady-state, but have been perturbed by the increase in greenhouse gases since pre-industrial times. A more reasonable steady-state would be one spun-up using pre-industrial greenhouse gas concentrations. Thus we run this second phase with the atmospheric radiative forcing for 1860 (e.g. atmospheric CO_2 of 286.4 ppmv). We run for 2000 years to allow the physical and carbon model to reach equilibrium. The air-sea flux of CO_2 is only one way – with the ocean carbon content allowed to change, but the atmospheric content kept constant. During this phase of the spin-up the long term average of air-sea flux of the carbon tends toward zero, so that the ocean is in steady-state with the pre-industrial carbon concentrations. The ocean heat content and circulation, and the feedbacks to and from the atmosphere also change to a pre-industrial steady-state.

In this phase, using a 3 GHz Pentium 4 chip, each year of model integration takes 14 minutes (the 4 additional minutes come from the ocean carbon cycle).

Phase 3: Once the model is in steady-state with the 1860 forcing, we start the third phase of the simulation. Here we force the model with observed changes in greenhouse gas concentrations (Hansen *et al.*, 2002), tropospheric ozone (Wang and Jacob, 1998), solar constant (Lean, 2000), sulfate (Smith *et al.*, 2004), and volcanic (Sato *et al.*, 1993) aerosols from 1860 to 1990. Natural emissions of methane and nitrogen are provided by Natural Emissions Model (NEM) and land uptake of carbon is determined by the Terrestrial Ecosystems Model (TEM).

The ocean is allowed to take up carbon, the atmospheric concentrations are however kept at the observed values (i.e. the ocean uptake does not affect the atmospheric CO_2 values). Although the ocean uptake is close to expected, the uptake by the land is somewhat less. We calculate the mismatch uptake to the expected 4.1 GtC y^{-1} for the 1980s. This mismatch is then used as a fixed correction for phase 4. The ocean circulation and carbon content changes to accommodate the additional radiative forcing as the greenhouse gas contents rise.

In this phase, using a 3 GHz Pentium 4 chip, each year of model integration takes 15 minutes (the additional minute comes from TEM/NEM).

Phase 4: After 1990, the model runs in fully coupled mode with all concentrations of gases and aerosols calculated by the atmospheric chemistry model. Ocean (and terrestrial) uptake does affect the atmospheric concentration. From 1990 to 1997, historical emissions are used, and after 1997 gases emissions are provided by the Emissions Prediction and Policy Analysis (EPPA) component of the IGSM2. The scenario described here is one of "business-as-usual" where there are no policy restrictions on emissions and EPPA uses predictions of population and economic growth to calculate future emissions.

The atmospheric chemistry and transport model leads to an additional 6 minutes per year of integration (on a 3 GHz Pentium 4 chip), so that in fully coupled mode the model takes 21 minutes per year.

4.2 Current Climate Results

How well does our coupled model perform? The model surface air temperature changes over the period 1860 to 2002 compare extremely well with the observations of Jones *et al.* (1999) (Fig. 9). Here we consider more fully the ocean/seaice/carbon model results from the later part of the 20th century and compare to observations. In general the model results compare favorably. We discuss the discrepancies more fully in the following sections.

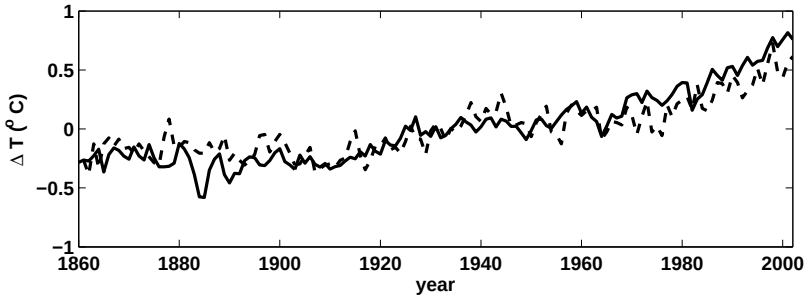

Figure 9: *Surface air temperature change from 1860 to 2002. Solid line is yearly averages from model with mean from period removed, dashed lines are observations (Jones et al., 1999) also with mean for the period removed.*

4.2.1 Ocean and Seaice Models

The 3-D ocean circulation model provides a reasonable circulation. The patterns of gyres and strong western boundary currents are apparent in the horizontal circulation (Fig. 10). The Antarctic Circumpolar Current (ACC) has maximum values of 100Sv, within the observed range of 100-120 Sv (Pickard and Emery, 1990; Nowlin and Klinck, 1986). Gyre circulations compare well to the 30-50 Sv found from observations (Leetmaa and Bunker, 1978). However, the North Atlantic surface flow does not go far enough north (in this example run there is no flux adjustments poleward of 60^o). This leads to surface temperatures in the North Atlantic being too low (Fig. 11a,b). Too much deep water formation in the Antarctic leads to deep temperatures also being too low (Fig. 11c,d). The deep Arctic is too warm, suggesting an Arctic circulation that is too sluggish. However, over all there is good agreement between the model temperature fields and observations. In particular the thermocline depths across the ocean (Fig. 11c,d) compare well with observations. Zonally integrated meridional heat transports (Fig. 12a), $\rho_{sw} c_p \int \int_{-H}^{0} v(x,y,z)\theta_o(x,y,z)dzdx$, show the general trend anticipated by the box-inverse model of hydrographic WOCE sections (Ganachaud and Wunsch, 2003). The northern transport at 20^oN may not be large enough and the southern transport at 20^oS may be too large, but the model results are still generally within the uncertainties of the inversion study. Not enough northward heat transport north of 40^oN is consistent with the problems with the ocean circulation in the northern North Atlantic.

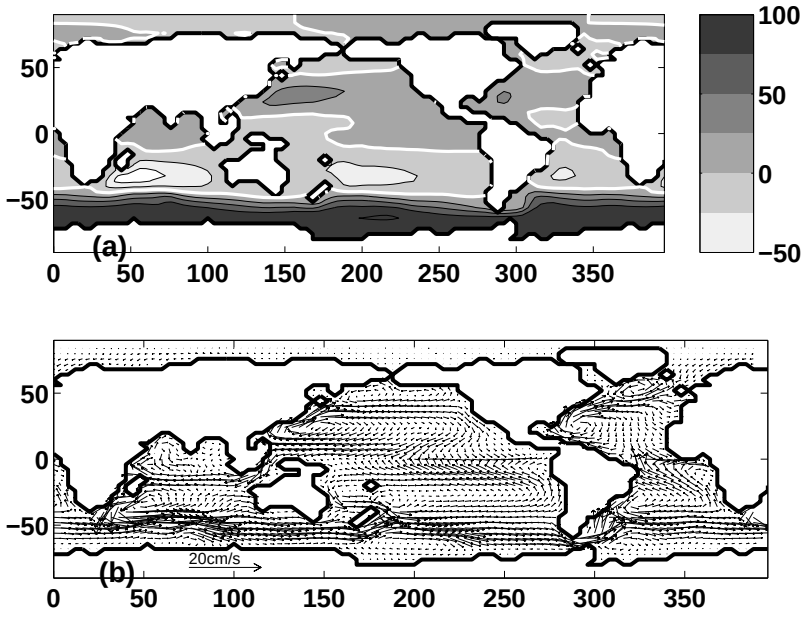

Figure 10: *Ocean model: (a) barotropic Stream Function (Sv); and (b) horizontal velocity (m* s^{-1}*) vectors at 85m. Model data is averaged over the years 1950 to 1990. Contour interval in (a) is 25 Sv.*

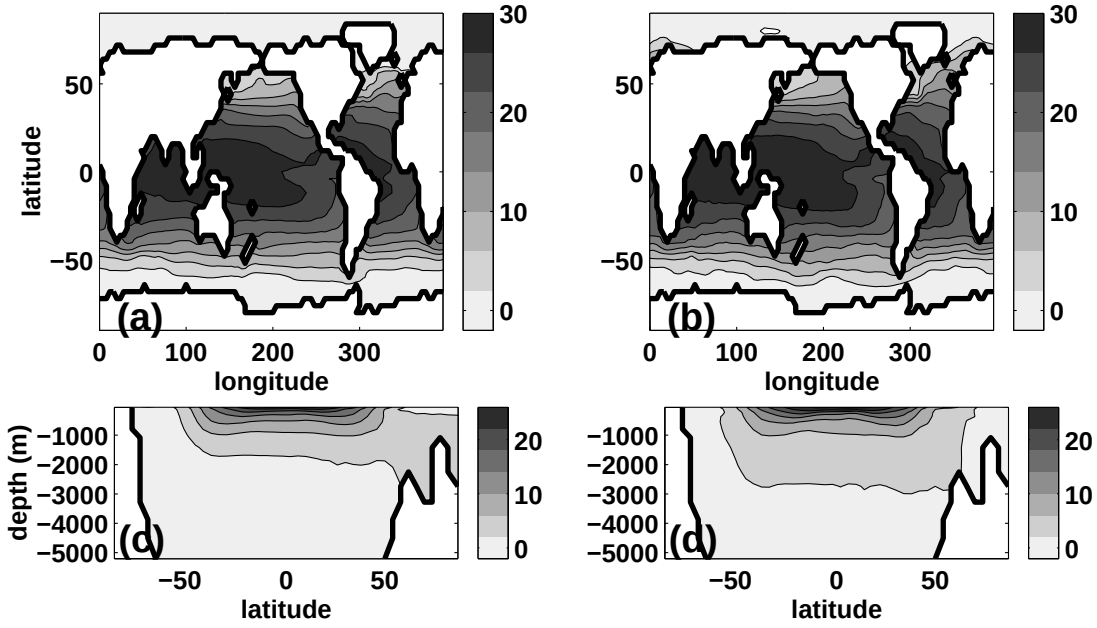

Figure 11: *Annual mean temperature (*$^o C$*) of surface layer (0-50m) of ocean (a) model, (b) observation. Global zonally averaged ocean temperature (*$^o C$*) transect of (c) model, (d) observation. Model results are from 1950 to 1990 and observations are from Levitus and Boyer (1994). Contour intervals are 4*$^o C$*.*

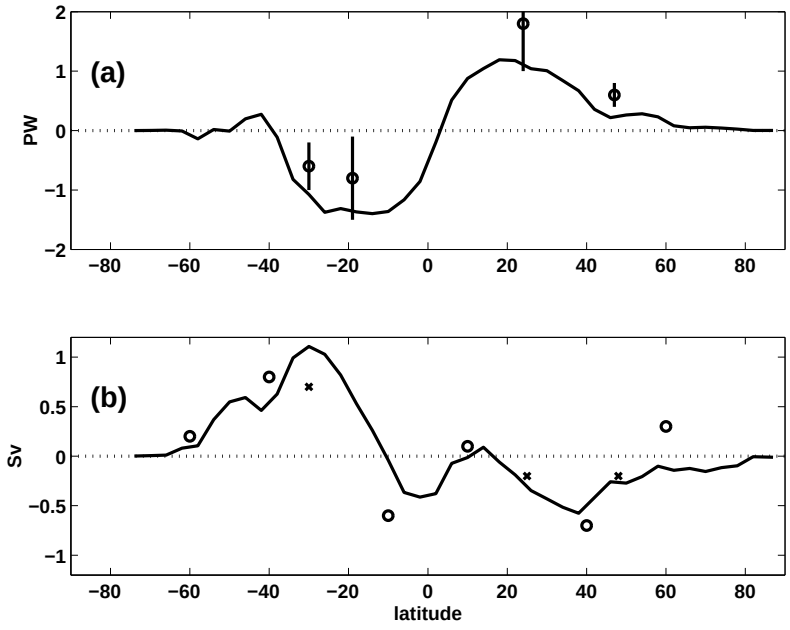

Figure 12: *Modelled zonally integrated meridional transport of: (a) heat (PW), and (b) freshwater (Sv), averaged from 1950 to 1990. In (a) circles are from Ganachaud and Wunsch (2003), with vertical line indicating uncertainty estimates; in (b) circles are from MacDonald and Wunsch (1996) and crosses from Wijffels et al. (1992).*

How well does the model capture changes to the observed ocean temperature over the last half of the 20th century? Levitus *et al.* (2005) observe a 0.037^oC change in ocean temperature (averaged from 0 to 3000m) between 1955 and 1998. Our coupled model finds 0.055^oC change. Levitus *et al.* (2005) find that most of the heat content increase occurs in the top 700 m. This is consistent with our model (Fig. 13). Our model trend matched the observations well through the early 1990s (albeit with a lower inter-annual variability), after which the model heat content change is slightly too large. Here heat content is defined as:

$$\rho_{sw} c_p \int \int \int_V \theta_o(x, y, z) dx dy dz.$$

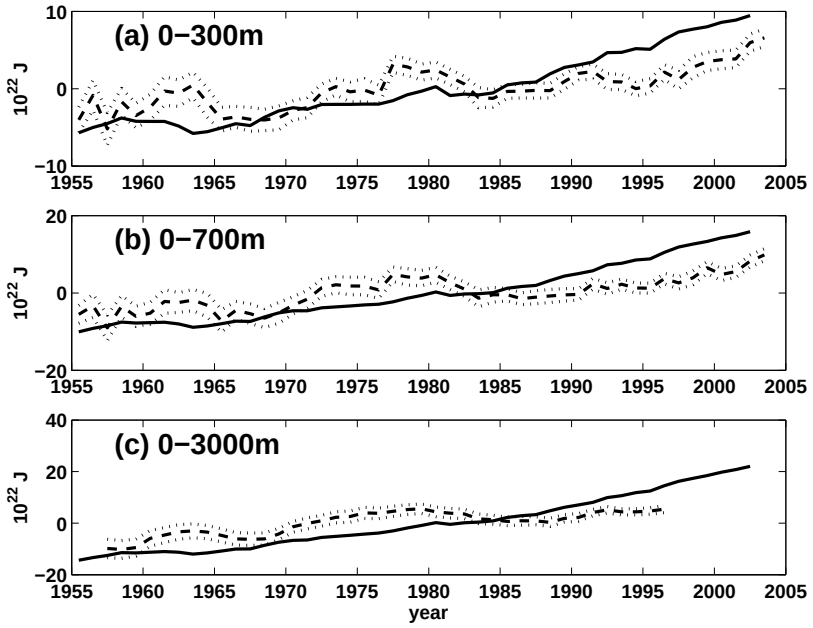

Figure 13: *Ocean heat content (10^{22} J) for the year 1955 to 2003: (a) 0-300 m; (b) 0-700 m; and (c) 0-3000 m. Solid line shows annual mean model data (with mean from the period removed), dashed line show observations (Levitus et al., 2005) and standard error (dotted line), also with mean for period removed. Observational data are annual means for (a) and (b) and five year averages for (c).*

The model salinity (Fig. 14) compare fairly well with observations. Some discrepancies, as with temperature, arise especially in the northern North Atlantic and Arctic oceans. Fresh water from river inflow in the Arctic is not dissipated enough, leading to low surface salinities in these parts. Some of this is probably due to the sluggish Arctic circulation and not enough influx of Atlantic water, but problems also arise from the runoff weighting function putting too much freshwater into the Arctic rivers. The deep Arctic becomes too salty. The zonally integrated meridional freshwater transport (Fig. 12b), $\rho_{sw} \int \int_{-H}^{0} v(x, y, z)(1 - \frac{S_o(x,y,z)}{S_*}) dz dx$, follows the trends found by MacDonald and Wunsch (1996) and Wijffels *et al.* (1992), although the maximum transport at 10^oS may be too low, and the northward transport poleward of 60^oN is not captured.

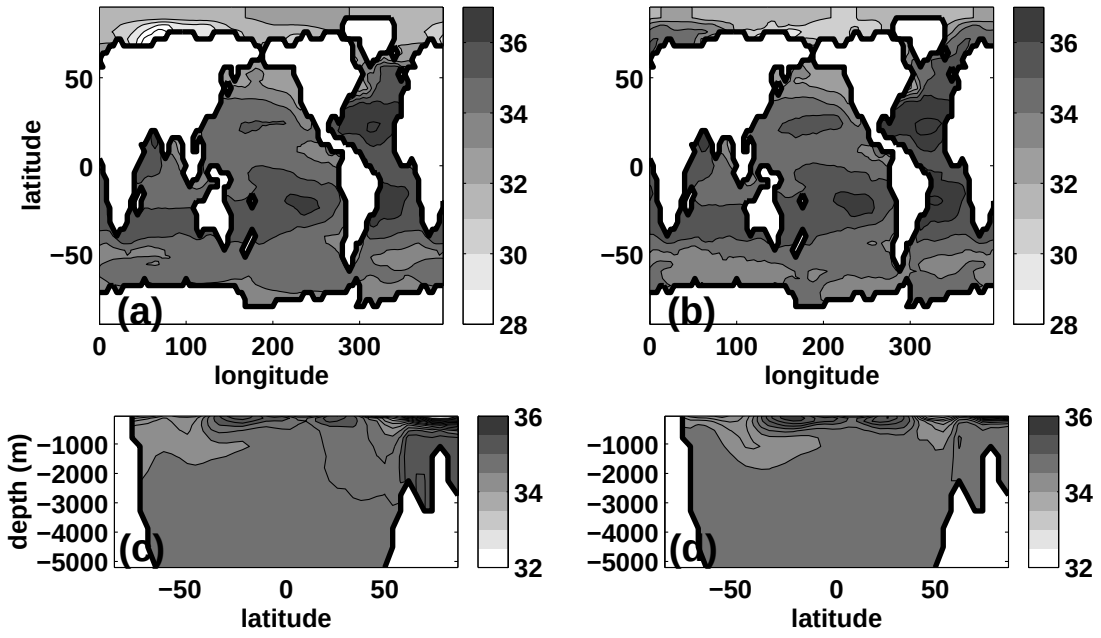

Figure 14: *Annual mean salinity (psu) of surface layer (0-50m) of ocean (a) model, (b) observation. Global zonally averaged ocean salinity (psu) transect of (c) model, (d) observation. Model results are from 1950 to 1990 and observations are from Levitus et al. (1994). Contour intervals are 1 psu for surfaces plots and 0.2 psu for transects.*

The meridional overturning circulation is also in good agreement with estimations from observations. Figure 15a shows the effective ("residual") zonally averaged overturning. This overturning includes contributions from the Eulerian transport and that due to the eddy parameterization. The upper (positive) overturning cell in the Southern Ocean has a maximum of 20 Sv, higher than 14 Sv inferred from transient tracers by Ito *et al.* (2004). The Atlantic effective overturning is plotted in Figure 15b. The maximum overturning in the North Atlantic is 15 Sv (13 Sv is the purely Eulerian part), in good agreement with that inferred from the inverse model of Ganachaud and Wunsch (2000)(15±2 Sv).

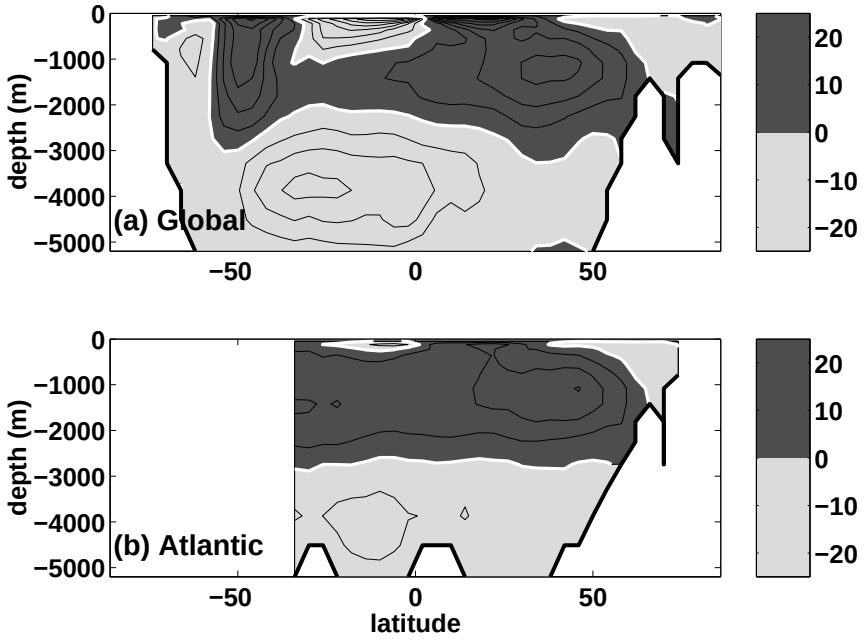

Figure 15: *Ocean model effective (including both Eulerian and eddy parts) overturning stream function (Sv) for: (a) Global, and (b) Atlantic. Dark shading denotes positive values, contour interval in 5Sv and zero contour is white. Model results are averaged over 1950 to 1990.*

The low sea surface temperatures in the North Atlantic allows too much seaice coverage in the Norwegian and Greenland seas (Fig. 16a,b). While seaice extent (defined as the total area of each grid cell with at least 20% covered by seaice) compares well, especially in the northern hemisphere, to observations obtained from passive microwave, the actual area of seaice is too large (Fig. 17). This suggests that the fractioning between seaice and open ocean in each grid cell is not captured well by the seaice model. In the northern hemisphere, the model seasonal cycle is reasonable, although there is too much ice (mostly in the Norwegian and Greenland seas). In the southern hemisphere, seaice area is reasonable in the winter, but does not melt enough in the summer. Ice heights are reasonable: average height in the Southern hemisphere is 3.3 m and 2.5 m in the Northern hemisphere.

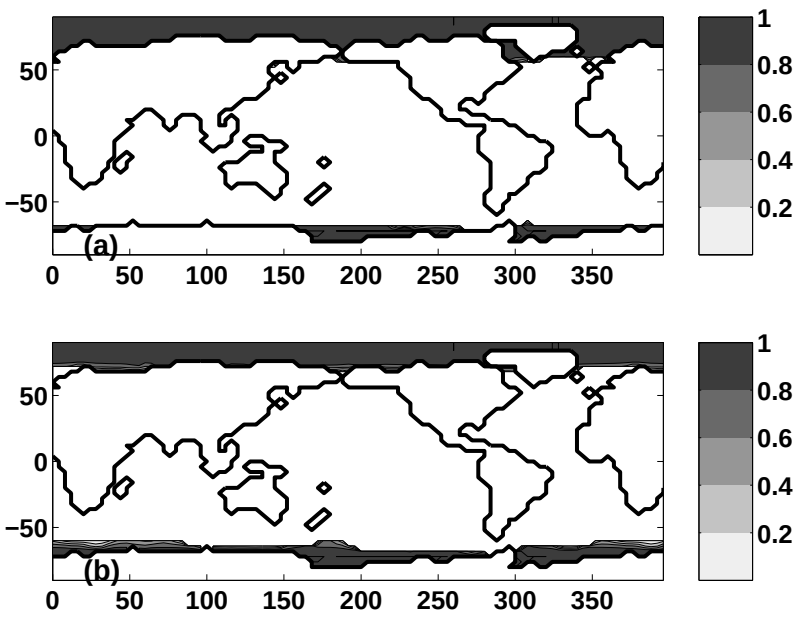

Figure 16: *Seaice coverage for 1980 (given as a fraction of the ocean grid) in (a) March; (b) September.*

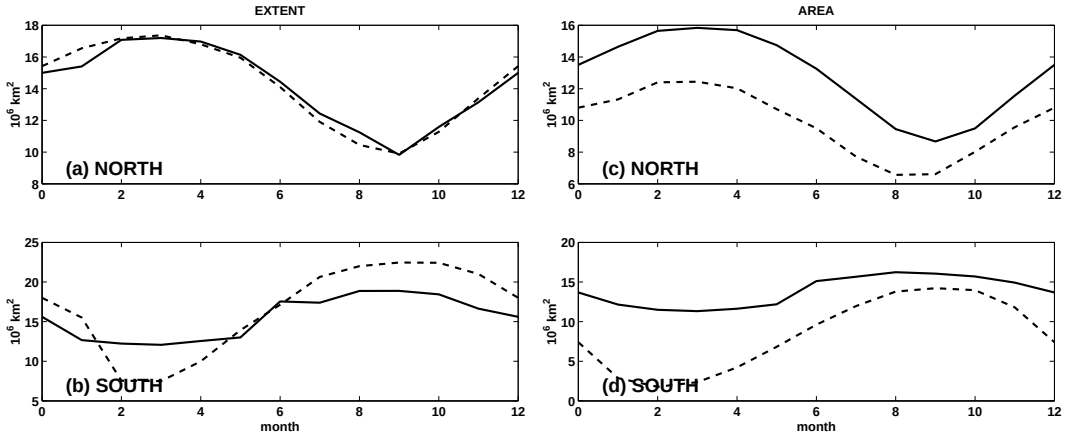

Figure 17: *Monthly averaged extent of ocean covered by seaice (million km^2) for the (a) northern hemisphere, (b) southern hemisphere; and area of ocean covered by seaice (million km^2) for the (c) northern hemisphere; and (d) southern hemisphere. Solid line indicates the model results and dashed line indicates those from NASA passive microwave observations (Cavalieri, 1992). Observations and model results from the 1980s.*

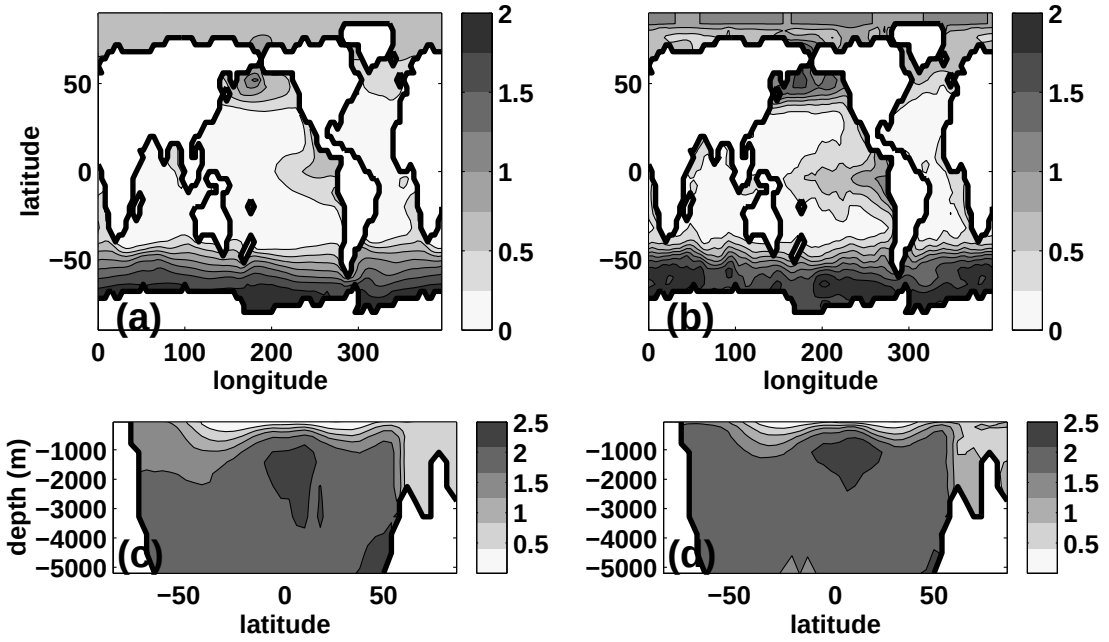

Figure 18: *Annual mean phosphate (μM) of surface layer (0-50m) of ocean (a) model, (b) observation. Global zonally averaged ocean phosphate (μM) transect of (c) model, (d) observation. Model results are averaged from 1950 to 2000 and observations are from Conkright et al. (2002). contour interval is 0.25 μM for (a) and 0.5 μM for (b).*

4.2.2 Ocean Carbon

The carbon model captures both the biological and solubility pumps of carbon into the ocean. The biological production parameterization accomplishes a reasonable pattern of export production, with elevated productivity in the upwelling regions of the ocean. The surface pattern of phosphate that emerges (Fig. 18a) compares favorably to that of observations (Fig. 18b). The slightly lower values in the equatorial and northern Pacific than in the observations are probably caused by the lack of iron limitation in our parameterization. Low iron in these regions tends to retard productivity and the uptake of nutrients, so observed phosphate is higher in these regions than might otherwise be expected. Since we do not model the effects of iron, we do not expect to be able to capture the distinction between these areas and other upwelling regions. The model nutricline also compares well to observations (Fig. 18c,d). However the upper Southern Ocean has too little phosphate, maybe indicative of problems with the deep Antarctic circulation.

The combination of the biological sinking of carbon and the air-sea exchange of CO_2 combine to provide the sea surface total dissolved organic carbon (Fig. 19a,b). The pattern of low values in tropical waters and higher values in ice-free higher latitude waters is captured by the model. Warm waters can hold less carbon, and tropical waters tend to out-gas to the atmosphere (Fig 20). Colder waters tend to uptake carbon. In our current climate (1990-2000), observations show that most of the higher latitudes are taking up CO_2, and this is

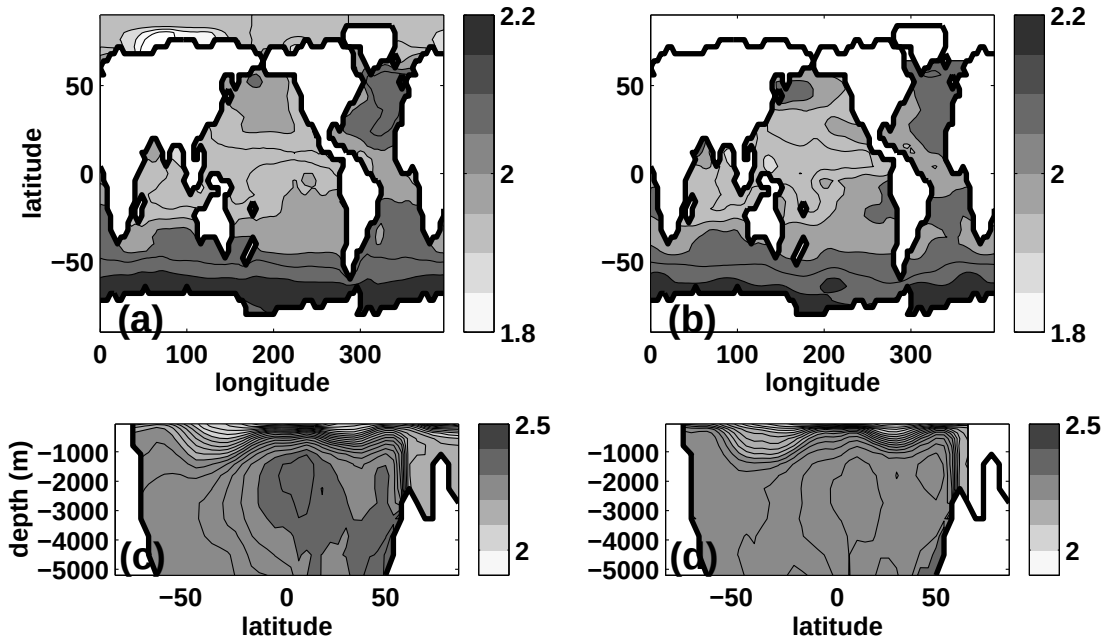

Figure 19: *Annual mean total dissolved carbon (mol m^3) of surface layer (0-50m) of ocean (a) model, (b) observation. Global zonally averaged ocean total dissolved carbon (mol m^3) transect of (c) model, (d) observation. Model results are averaged from 1990 to 2000 and observations are from Key et al. (2004). The observational data set does not have data in the Arctic. Contour intervals are 0.05 mol m^3 for (a) and 0.02 mol m^3 for (b).*

indeed captured in our model (Fig 20). However the model results tend to be smoother than the observations (indicative of the low resolution) and some of the very strong out-gassing observed in the equatorial regions is not captured. Our model biological production in the equatorial regions is too strong, owing to the lack of iron limitation, leading to excessive sinking of carbon, and thus a air-sea disequilibrium of CO_2 that is too low.

The deep ocean tends to sequester carbon. Sinking organic matter takes carbon away from the surface, enhancing the vertical gradient of carbon and modifying the air-sea fluxes. The sinking material leads to higher carbon concentrations at depth. This process is captured by our model (Fig. 19c,d). Our model has an ocean carbon content increase of 3% from pre-industrial through the 20th century – in good agreement with the estimates from observations (Key *et al.*, 2004).

4.3 Future Climate Scenario

Our model does a reasonable job of capturing the modern day ocean properties and 20th century changes. How will this model respond to future changes to the atmospheric increase in greenhouse gases?

The transient response of the coupled model to a given forcing is, to large extent, defined by the model "climate sensitivity" and the rate of heat uptake by the deep ocean. Climate

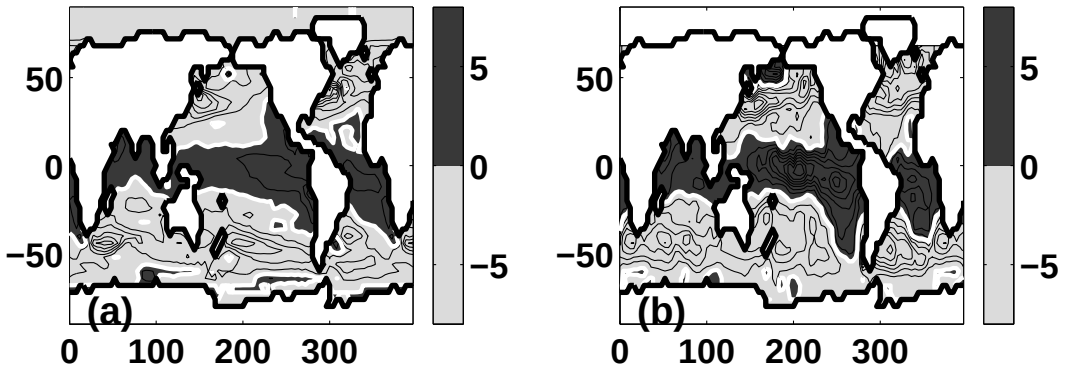

Figure 20: *Annual mean air-sea flux of CO_2 (mol C m^{-2} y^{-1}) for (a) model and (b) observations. Model results are from 1990 to 2000, the same time average for the observations (Takahashi et al., 2002). Dark shading indicates out-gassing, contour interval is 1 mol C m^{-2} y^{-1}. The Takahashi et al. (2002) observations has no data in the Arctic.*

sensitivity is usually defined as the equilibrium surface warming simulated by an atmospheric model coupled to a mixed layer ocean model in response to the doubling of atmospheric CO_2 concentrations. However a number of studies (e.g. Raper *et al.*, 2002; Sokolov *et al.*, 2003) have shown that transient climate change simulated by coupled atmosphere/ocean models is better described by an effective climate sensitivity (S_{eff}, which can determined from the results of transient runs, see for example Sokolov *et al.*, 2003). It was also shown by Sokolov *et al.* (2003) that results produced by coupled AOGCMs can be matched by a version of the IGSM which includes a diffusive mixed layer ocean model (rather than the 3D model discussed in this report). The "effective diffusion coefficient" (K_v) for ocean heat anomalies from the diffusive model can then be used as a measure of the heat uptake by the 3D ocean models. The S_{eff} of our coupled model estimated from a simulation with 1% per year increase in CO_2 concentration is 2^oC. Long term simulations carried out for IPCC AR4 showed that equilibrium sensitivity of our model is also 2^oC. The K_v required by the diffusive mixed layer ocean model to match the transient surface warming and sea level rise due to thermal expansion of the deep ocean simulated in the 3D model was 4 cm^2 s^{-1}. Both S_{eff} and K_v are near the low end of the ranges obtained for coupled AOGCMs used in CMIP2 simulations (Sokolov *et al.*, 2003).

The 4th phase of this model simulation uses predictions of anthropogenic emissions through the 21st century. The changes in the radiative forcing work to increase the surface temperatures and decrease seaice cover. Higher atmospheric CO_2 and changes to ocean biological production and circulation lead to changes in the ocean carbon inventories. We stress here that this is just one model result, with one set of parameters. A fuller investigation of the uncertainties in the model parameters (e.g. vertical diffusion, cloud feedback), the uncertainties imposed by the model structure and coupling mechanisms, as well as the uncertainties in future emission predictions need to be addressed before we can ascertain a likelihood of the following scenario occurring. However, to give a full description of the current example simulation, we discuss further some of the results from phase 4.

In fully coupled mode, the model predicts that in a world where there are no new policies on emissions, and with projected population and economic growth, the atmospheric CO_2 concentrations will increase from 352 ppmv in 1990 to 956 ppmv in 2100 (Fig. 21a). The climate system responds with an increase in surface air temperatures of about 4^oC (between 1990 and 2100) and the global sea surface temperature increases by 2.7^oC (Fig. 21b,c). The increase in sea surface is not uniform, but more pronounced in the northern hemisphere (Fig. 22). In areas where there is still ice coverage much of the year in 2100, there is very little change in sea temperature. The ocean takes up 2.8×10^{24} J of heat between 1990 and 2100 (Fig. 21d). The increase in the ocean temperatures leads to a sea level rise of 32 cm between 1990 and 2100 (Fig. 21e). This rise is only from thermal expansion (the effects of land ice melt are not taken into account).

Increased air and sea surface temperatures lead to a melting of some of the seaice. The coupled model predicts a 25% decrease in the maximum seaice extent between 1990 and 2100 (Fig. 21f), a 30% decrease in the annual average seaice area and 44% decrease in annual average seaice mass. (Here, "extent" refers to the area of all grid cells with 20% or greater ice fraction; "area" refers to the exact area of ocean covered with seaice; "mass" is ice area multiplied by ice height, divided by density of ice). This means that everywhere the seaice height will decrease, and in many areas it will disappear completely. Loss of seaice area will lead to a decrease in the surface albedo, producing a positive feedback to warming.

A warming, freshening North Atlantic leads to a slowing down of the meridional overturning circulation: the maximum decreases from 14.9 Sv in 1990 to 8.1 by 2100 (Fig. 21g). This will decrease the rate with which the ocean can take up excess heat, and therefore is also a positive feedback to warming.

With anthropogenic perturbation, the ocean begins to take up carbon dioxide (Fig. 23a). The average ocean carbon uptake in the model between 1990 and 2000 1.88 GtC y^{-1}, slightly higher than the value (1.7 GtC y^{-1}) estimated by the IPCC Report (2001) for this period. Over the course of the first part of the 21st century, the model predicts that the ocean will increase its uptake of CO_2 almost linearly. However, after 2050, the ocean uptake levels off. It is still taking up carbon dioxide, but at a fairly constant rate of 5.2 GtC y^{-1}. Why this maximum uptake? Figure 24 shows four different 10-year averages of air-sea flux of CO_2. It is interesting to note how different today (1990-2000) ocean uptake is from pre-industrial times. In pre-industrial times, the Southern Ocean actually out-gassed carbon dioxide. Water with high carbon content upwells into this region (see Fig. 19), and with atmospheric concentrations of 286.4 ppmv, the dis-equilibrium drove CO_2 back into the atmosphere. By the end of last century, we had already altered this pattern. With 350 ppmv in the atmosphere, the southern ocean, even with its high DIC concentrations became a sink for carbon. Over the course of the 21st century, more portions of the surface ocean become sinks. By the end of the century almost all of the surface ocean is a carbon sink. Most of the increase in uptake seen in the first half of the 21st century came from regions switching from out-gassing to sinks. Once most of the ocean surface is a sink, the uptake levels off. The ocean inventory of carbon still continues to rise with this constant uptake (Fig. 23b), so that the ocean has 435 Gt more carbon in it by the year 2100 than there was in 1990. The anthropogenic CO_2 is diffused and advected into the deeper ocean. In addition a portion sinks to depth as biological matter.

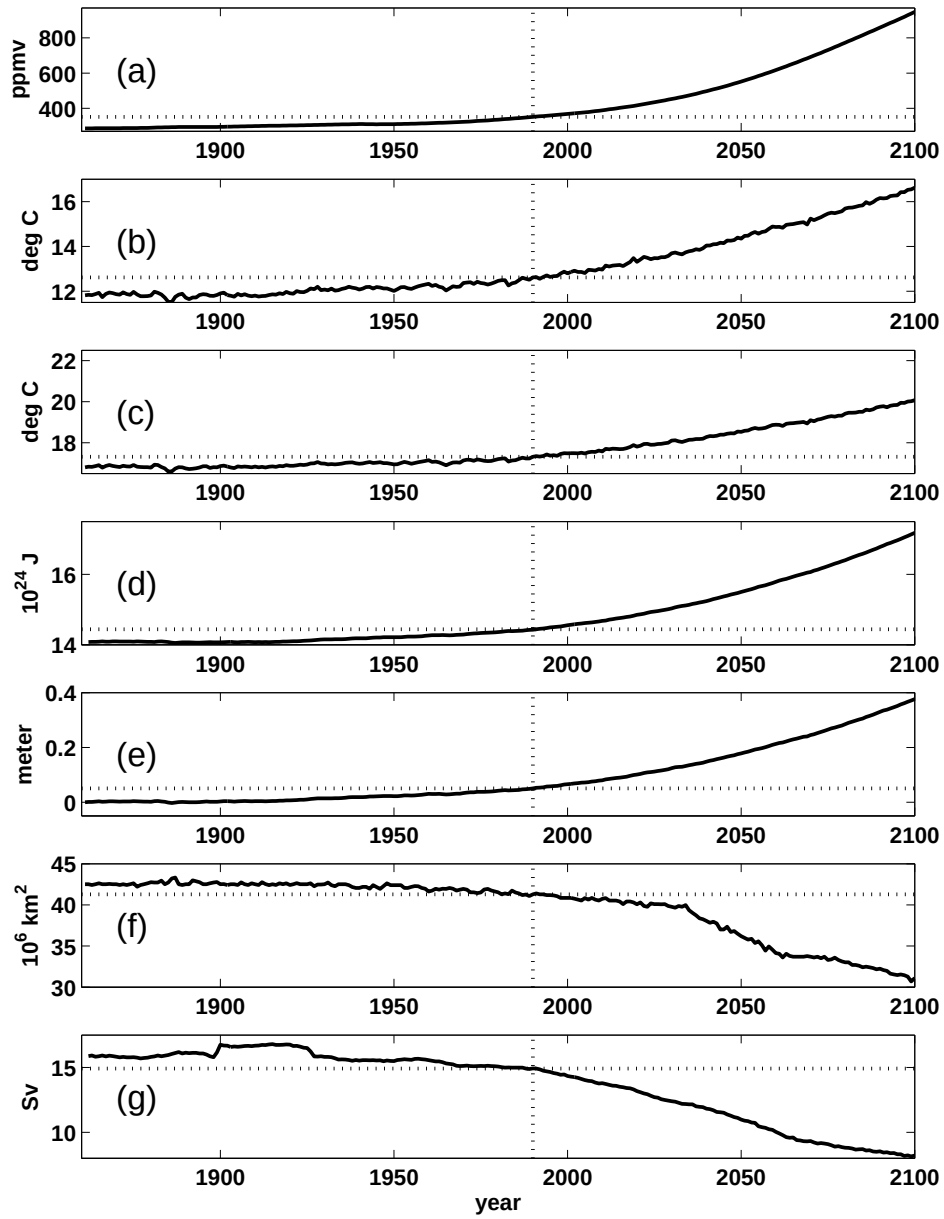

Figure 21: *Model global: (a) atmospheric pCO_2 (ppmv); (b) surface air temperature (^oC); (c) sea surface temperature (^oC); (d) ocean heat content (10^{24} J); (e) sea level rise (m) relative to 1860; (f) sea ice extent (million km^2); (g) maximum North Atlantic overturning (Sv). Atmospheric pCO_2 is provided by observed values from 1860 to 1997; and are predicted by full IGSM2 from 1998 to 2100. Sea level rise is due only to thermal expansion of the ocean water, and does not include rise due to the melting of ice. Dotted lines give values at 1990.*

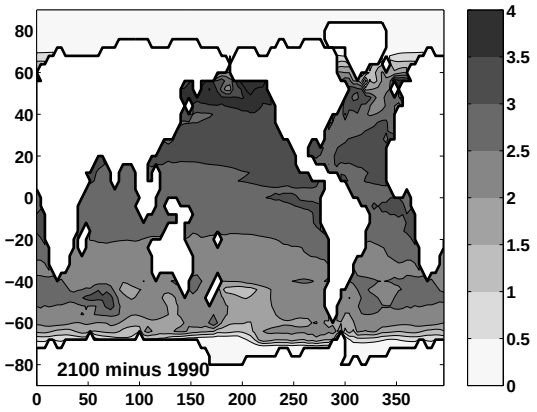

Figure 22: *Difference in SST (^oC) between decades 1990 to 2000 and 2090 to 2100. Contour interval is 0.5^oC.*

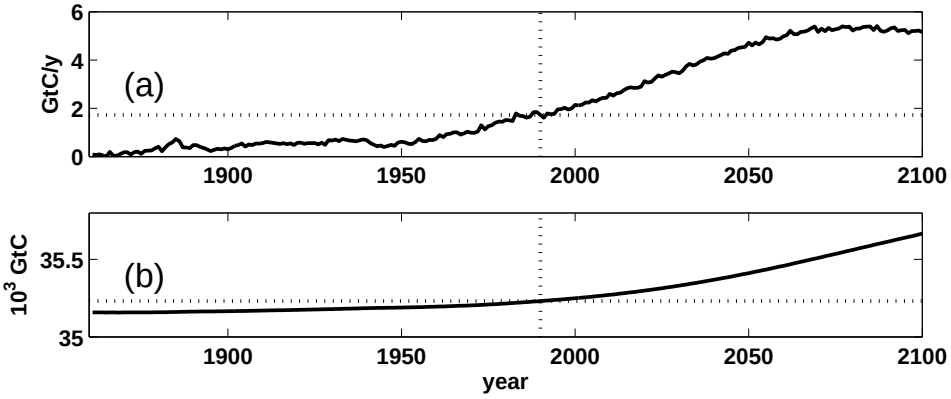

Figure 23: *Model global: (a) air-sea flux of CO_2 ($GtC\ y^{-1}$); (b) ocean inventory of carbon (10^3 GtC).*

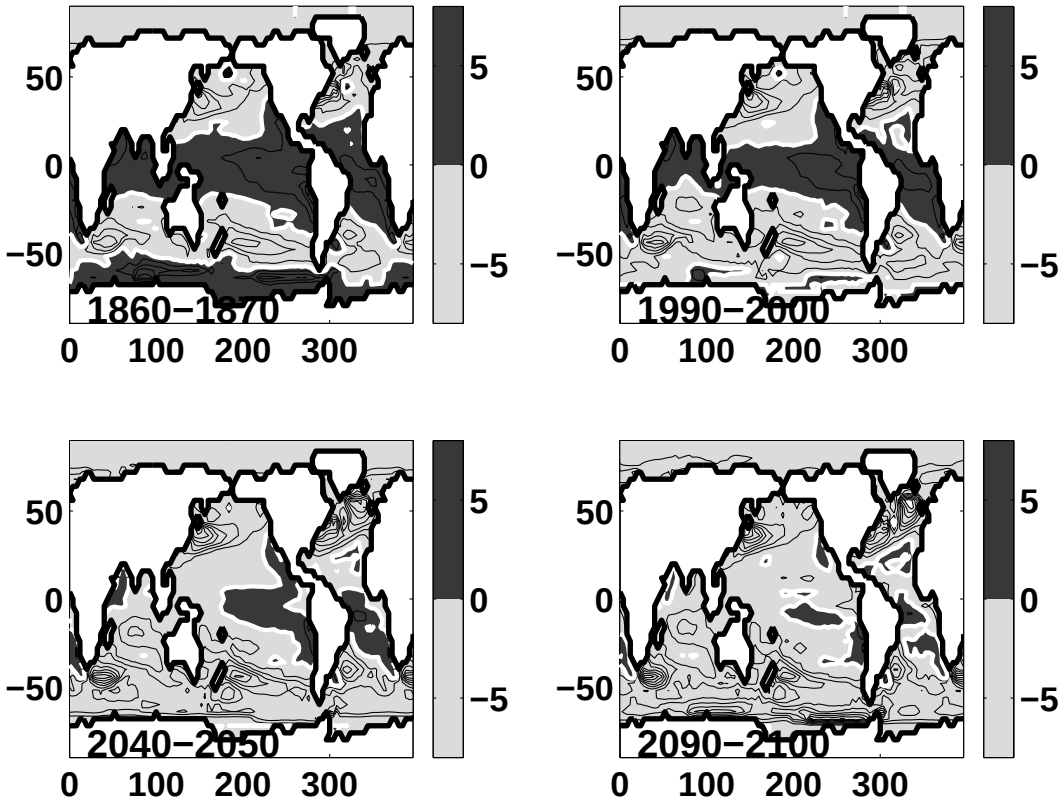

Figure 24: *Ten year averages of air-sea flux of CO_2 (mol C m^{-2} y^{-1}): (a) 1860 to 1870; (b) 1990 to 2000; (c) 2040 to 2050; (d) 2090 to 2100. Positive values (dark shading) indicate out-gassing of CO_2 from the ocean to the atmosphere.*

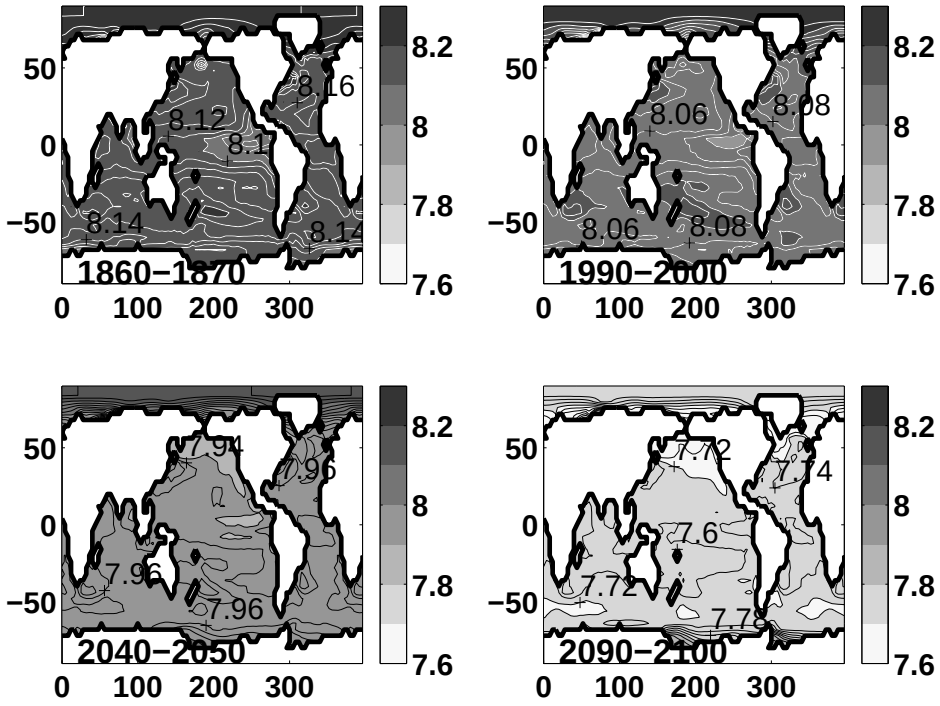

Figure 25: *Ten year averages of sea surface pH: (a) 1860 to 1870; (b) 1990 to 2000; (c) 2040 to 2050; (d) 2090 to 2100. Contour interval is 0.02, white contours indicate values 8 or greater, black contours indicate less than 8.*

The additional carbon in the ocean leads to a more acidic ocean. In fact the pH of the surface ocean has changed, and will change even more dramatically over the course of this century (Fig. 25). On average the pH will decrease by 0.3 by 2100. This will cause problems for some marine organisms (e.g. coccolithophores) which form calcium carbonate shells. Such shells will actually "dissolve" in more acidic water. This change to the biological productivity of the ocean is not addressed in this model, and should be the direction of future research.

We have seen above, that the solubility pump changes dramatically. How does our model biological productivity change in this simulation? How about the biological pump? We find that there is 14% decrease in the export production in the model between 1990 and 2100. The decrease occurs over much of the ocean, except in the regions where seaice coverage decreases (Fig. 26). Seaice prevents sunlight from reaching the surface waters. In regions where there is less seaice in 2100, productivity increases. However over most of the ocean, increased stratification leads to a decrease in the amount of macro-nutrients that reach the surface and productivity decreases. It is not clear, however, whether this will lead to a decrease in the biological pump, as the efficiency of the pump is dictated by both productivity and the rate at which deep carbon is ventilated to the surface (Parekh *et al.*, 2005). An investigation of this will continue in future studies.

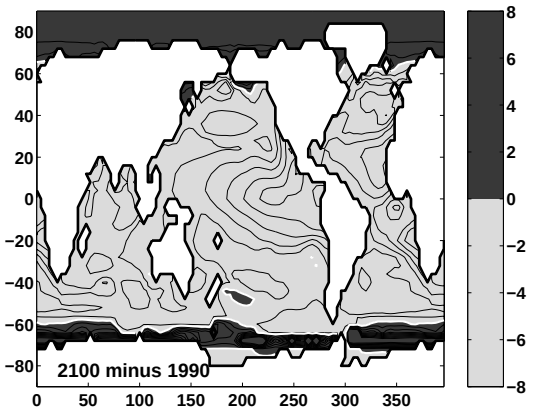

Figure 26: *Change in export production (gC m^{-2} y^{-1}) through 50 m between 2100 and 1990. Light shading shows negative values where export decreases between 1900 and 2100, dark shading shows positive values where export increases. Contour interval is 1 gC m^{-2} y^{-1}.*

5 SUMMARY AND FUTURE PLANS

We have described the coupling of the two-dimensional atmospheric model to a three-dimensional ocean model. The ocean model has explicit representations of seaice and the carbon cycle. These additions make this coupled model an effective tool with which to investigate future climate scenarios and uncertainties.

The model is fairly efficient to run: on a Pentium 4, 3 GHz CPU and in the example run (Section 4) the fully coupled setup takes 21 minutes per year of integration (3 minutes for atmosphere, 4 in land hydrography, 3 in ocean/seaice, 4 in ocean carbon cycle, 1 in NEM/TEM, 6 in atmospheric chemistry). With this speed many 20th and 21st century simulations can be accomplished. These simulations can be used to ascertain model uncertainties. However, the coupled system is flexible and various components can be turned on and off. As a very efficient climate model neglecting chemistry, the coupled model can be run with only atmosphere and ocean/seaice physics at 6 minutes a year of integration (on a 3 GHz Pentium 4 chip).

An example simulation shows that the coupled model can provide a realistic looking ocean, seaice and ocean carbon cycle. Changes to the model surface air temperature, heat content, and carbon content over the 20th century compare well to observations. This example simulation, therefore, is a credible platform with which to look at future predictions of climate change. In a single scenario, where anthropogenic emissions of greenhouse gases increase with population and economic growth, and are unchecked by policies, the coupled model predicts air temperature changes of 4^{o}C over the 21st century. The ocean works as a heat and carbon sink, reducing some of the impact on the terrestrial system. However, ocean circulation does change in response, as does the carbon uptake both by solubility and biology. The feedbacks from these changes need to be examined in more detail. Such modifications can not be captured in our earlier 2-D ocean, hence this system is an improvement over the IGSM1. In particular, simulations past the end of the 21st century (e.g. atmospheric

pCO_2 stabilization scenarios) can not be accomplished with that 2-D ocean, as the ocean feedbacks become important (Sokolov *et al.*, 2005). The model described here is being used in several such stabilization simulations.

There are still uncertainties involved with the specific coupling mechanisms between the ocean and the 2-D atmosphere that need to be examined in more detail. The setup described in this report is flexible and a series of studies of different combinations of coupling is under investigation. Specifically we are addressing the uncertainties behind the freshwater fluxes, and the impact of either using the best observations or constraining the model to have reasonable sea surface salinities.

We plan to use this model to investigate the sensitivity of results to changes in vertical diffusion – a parameterization that likely dominates the uptake of heat by the ocean. However, the rate of the meridional overturning will also affect uptake and we will consider the impact of these two processes in future studies.

We are investigating the changes to the ocean circulation (for instance the North Atlantic overturning) for various emission scenarios. Specifically we are interested in the probabilities of an abrupt shut down of the overturning that could lead to even more drastic changes to the climate.

Further studies are planned for investigating the changes to the ocean carbon cycle. We plan to tease apart the impacts of climate change on the solubility and biological pumps. How important is the predicted decrease in ocean biological productivity on the ocean ability to store carbon?

6 REFERENCES

Babiker, M., J. Reilly, M. Mayer, R. Eckaus, I. Sue Wing, and R. Hyman, 2001: The emissions prediction and policy analysis (EPPA) model: Revisions, sensitivity, and comparison results, *Joint Program on the Science and Policy of Global Change Report*, 71, MIT, Cambridge, MA.

Bitz, C.M. and W.H. Lipscombe, 1999: An Energy-Conserving Thermodynamic Model of Sea Ice. *Journal of Geophysical Research*, 104, 15,669 – 15,677.

Bonan, G.B., K.W. Oleson, M. Vertenstein, S. Lewis, X. Zeng, Y. Dai, R.E. Dickinson, and Z.-L. Yang, 2002: The land surface climatology of the Community Land Model coupled to the NCAR Community Climate Model, *Journal of Climate*, 15, 3123–3149.

Cavalieri, D.J., ed., 1992: *NASA Sea Ice Validation Program for the Defense Meteorological Satellite Program Special Sensor Microwave Imagery: Final Report*, NASA Technical Memorandum 104559, Washington, D.C., 126pp.

Conkright, M.E., H.E. Garcia, T.D. O'Brien, R.A. Locarnini, T.P. Boyer, C. Stephens J.I. Antonov, 2002: *World Ocean Atlas 2001, Volume 4: Nutrients*, in *NOAA Atlas NESDIS*, 52, U.S. Government Printing Office, Washington, D.C.

Dai, Y., X. Zeng, R.E. Dickinson, I. Baker, G. Bonan, M. Bosilovich, S. Denning, P. Dirmeyer, P. Houser, G. Niu, K. Oleson, A. Schlosser, and Z.-L. Yang, 2003: The Common Land Model (CLM), *Bulletin of the American Meteorological Society*, 84, 1013–1023.

Dalan, F., P.H. Stone and A.P. Sokolov, 2005: Sensitivity of ocean's climate to diapycnal diffusivity in EMIC. Part II: Global warming scenario, *Journal of Climate*, 18, 2482–2496.

DOE, 1994: *Handbook of methods for the analysis of various parameters of the carbon dioxide system in sea water (Version 2)*, A.G. Dickson and C. Goyet (eds), ORNL/CDIAC-74.

Felzer B., D.W. Kicklighter, J.M. Melillo, C. Wang, Q. Zhuang, and R.Prinn, 2004: Effects of ozone on net primary production and carbon sequestration in the conterminous United States using a biogeochemistry model, *Tellus*, 56B, 230–248.

Forest, C.E., P.H. Stone, A.P. Sokolov, M.R. Allen, and M. Webster, 2002: Quantifying uncertainties in the climate system properties with the use of recent climate observations, *Science*, 295, 113–117.

Ganachaud, A. and C. Wunsch, 2003: Large-scale ocean heat and freshwater transports during the World Ocean Circulation Experiment. *Journal of Climate*, 16, 696–705.

Ganachaud, A. and C. Wunsch, 2000: The oceanic meridional overturning circulation, mixing, bottom water formation and heat transport, *Nature*, 408, 453 – 457.

Gent, P. and J. McWilliams, 1990: Isopycnal mixing in ocean circulation models. *Journal of Physical Oceanography*, 20, 150 – 155.

Gerdes, R., C. Koberle, A. Beckmann, P. Herrmann and J. Willebrand, 1999: Mechanisms for spreading of Mediterranean water in coarse-resolution numerical models. *Journal of Physical Oceanography*, 29, 1682 – 1700.

Hansen, J., M. Sato, L. Nazarenko, R. Ruedy, A. Lacis, D. Koch, I. Tegen, T. Hall, D. Shindell, B. Santer, P. Stone, T. Novakov, L. Thomason, R. Wang, Y. Wang, D. Jacob, S. Hollandsworth, L. Bishop, J. Logan, A. Thompson, R. Stolarski, J. Lean, R. Willson,

S. Levitus, J. Antonov, N. Rayner, D. Parker, and J. Christy, 2002: Climate forcings in Goddard Institute for Space Studies SI2000 simulations, *Journal of Geophysical Research*, 107, 4347.

Hansen, J., G. Russell, D. Rind, P. Stone, A. Lacis, S. Lebedeff, R. Ruedy, and L. Travis, 1983: Efficient three-dimensional global models for climate studies: Models I and II, *Monthly Weather Review*, 111, 609–662.

Huang, B., P.H. Stone, A.P. Sokolov, and I.V. Kamenkovitvh, 2003: The deep-ocean heat uptake in transient climate change, *Journal of Climate*, 16, 1352–1363.

Intergovernmental Panel on Climate Change, working group I, 2001: *Climate change 2001. The scientific basis*, Houghton, J. T., et al., eds., Cambridge University Press, UK.

Ito, T., J. Marshall, and M.J. Follows, 2004: What controls the uptake of transient tracers in the southern ocean? *Global Biogeochemical Cycles*, 18, doi:10.1029/2003GB002103.

Jones, P.D., M. New, D.E. Parker, S. Martin, and I.G. Rigor, 1999: Surface air temperature and its changes over the past 150 years, *Reviews of Geophysics*, 37, 173–199.

Kamenkovich, I.V., A.P. Sokolov, and P.H. Stone, 2002: An efficient climate model with a 3D ocean and statistical-dynamical atmosphere, *Climate Dynamics*, 19, 585–598.

Key, R.M., A. Kozyr, C.L. Sabine, K. Lee, R. Wanninkhof, J. Bullister, R.A. Feely, F.J. Millero, C. Mordy, T.-H. Peng, 2004: A global ocean carbon climatology: Results from GLODAP, *Global Biogeochemical Cycles*, 18, GB4031, doi:10.1029/2004GB002247.

Large, W.G., J.C. McWilliams, and S.C. Doney, 1994: Oceanic vertical mixing: A review and a model with a nonlocal boundary layer parameterization, *Reviews of Geophysics*, 32, 363–403.

Lean, J., 2000: Evolution of the Sun's Spectral Irradiance Since the Maunder Minimum, *Geophysical Research Letters*, 27, 2421-2424.

Leetmaa, A. and B.F. Bunker, 1978: Updated charts of mean annual wind stress, convergences of Ekman layers, and Sverdrup transports in North Atlantic, *Journal of Marine Research*, 36, 311-322.

Levitus, S. and T.P. Boyer, 1994: *World Ocean Atlas 1994 Volume 4: Temperature*, NOAA Atlas NESDIS 4, U.S. Department of Commerce, Washington, D.C., 117pp.

Levitus, S., J. Antonov, and T.P. Boyer, 2005: Warming of the world ocean, 1955-2003, *Geophysical Research Letters*, 32, LO2604, doi:10.1029/2004GL021592.

Levitus, S., R. Burgett, and T.P. Boyer, 1994: *World Ocean Atlas 1994 Volume 3: Salinity*, NOAA Atlas NESDIS 3, U.S. Department of Commerce, Washington, D.C., 99pp.

Liu, Y., Modeling the emissions of nitrous oxide and methane from the terrestrial biosphere to the atmosphere, 1996: *Joint Program on the Science and Policy of Global Change Report*, 10, MIT, Cambridge, MA.

MacDonald, A.M. and C. Wunsch, 1996: An estimate of the global ocean circulation and heat fluxes, *Nature*, 382, 436–439.

Marshall, J.C., C. Hill, L. Perelman and A. Adcroft 1997a: Hydrostatic, quasi-hydrostatic and non-hydrostatic ocean modeling. *Journal of Geophysical Research*, 102, 5,733 – 5,752.

Marshall, J.C., A. Adcroft, C. Hill, L. Perelman, and C. Heisey, 1997b: A finite-volume, incompressible Navier-Stokes model for the studies of the ocean on parallel computers. *Journal of Geophysical Research*, 102, 5,753 – 5,766.

Matsumoto, K., J. L. Sarmiento, R. M. Key, O. Aumont, J. L. Bullister, K. Caldeira, J.-M. Campin, S. C. Doney, H. Drange, J.-C. Dutay, M. Follows, Y. Gao, A. Gnanadesikan, N. Gruber, A. Ishida, F. Joos, K. Lindsay, E. Maier-Reimer, J. C. Marshall, R. J. Matear, P. Monfray, A. Mouchet, R. Najjar, G.-K. Plattner, R. Schlitzer, R. Slater, P. S. Swathi, I. J. Totterdell, M.-F. Weirig, Y. Yamanaka, A. Yool, and J. C. Orr. 2004: Evaluation of ocean carbon cycle models with data-based metrics, *Geophysical Research Letters*, 31, L07303, doi:10.1029/2003GL018970.

McAvaney, B. J., et al, 2001: Model Evaluation, In *Climate Change 2001: The Scientific Basis*, Houghton, J. T., et al., eds., Cambridge University Press, Cambridge, UK, 471-524.

McKinley, G., M.J. Follows and J.C. Marshall, 2004: Mechanisms of air-sea CO_2 flux variability in the Equatorial Pacific and the North Atlantic. *Global Biogeochemical Cycles*, 18, doi:10.1029/2003GB002179.

Melillo, J.M., A.D. McGuire, D.W. Kicklighter, B.Moore III, C.J. Vorosmarty, and A.L. Schloss, 1993: Global climate change and terrestrial net primary production, *Nature*, 363, 234–240.

Millero, F., 1995: Thermodynamics of the carbon dioxide system in the oceans. *Geochemica et Cosmochimica Acta*, 59, 661–677.

Najjar, R. and J. Orr, 1998: Design of OCMIP-2 simulations of chlorofluorocarbons, the solubility pump and common biogeochemistry, http://www.cgd.ucar.edu/oce/klindsay/OCMIP/design.pdf.

Nowlin, W.D. Jr., and J.M. Klinck, 1986: The physics of the Antarctic Circumpolar Current, *Reviews of Geophysics*, 24, 469-491.

Parekh, P., M. Follows, S. Dutkiewicz, and T. Ito, 2005: Physical and biological regulation of the ocean carbon pump, *Paleoceanography*, submitted.

Perry, G.D., P.B. Duffy, and N.L. Miller, 1996: An extended data set of river discharges for validation of general circulation models, *Journal of Geophysical Research*, 101, 21339-21350.

Pickard, G.L. and W.J. Emery, 1990: *Descriptive Physical Oceanography*, Pergamon Press, Exeter, U.K. 320pp.

Prinn, R.G., H.D. Jacoby, A.P. Sokolov, C. Wang, X. Xiao, Z.L. Yang, R.S. Eckaus, P.H. Stone, A.D. Ellerman, J.M. Melillo, J. Fitzmaurice, D.W. Kicklighter, G.L. Holian, and Y. Liu, 1999: Integrated global system model for climate policy assessment: Feedbacks and sensitivity studies, *Climatic Change*, 41, 469–546.

Raper, C.S.B., J.M. Gregory, and R.J. Stouffer, 2002: The Role of Climate Sensitivity and Ocean Heat Uptake on AOGCM Transient Temperature and Thermal Expansion Response, *Journal of Climate*, 15, 124-130.

Roe, P.L., 1985: Some contributions to the modeling of discontinuous flows, In *Large-scale computations in fluid mechanics*, Eds. B.E. Engquist, S. Osher, and R.C.J. Somerville, American Mathematical Society, Providence R.I.

Sarmiento, J.L., G. Theile, R.M. Key, and W.S. Moore, 1990: Oxygen and nitrate new production and remineralization in the North Atlantic, *Journal of Geophysical Research*, 95, 18303 – 18315.

Sato, M., J.E. Hansen, M.P. McCormick, and J.B. Pollack, 1993: Stratospheric aerosol optical depths, *Journal of Geophysical Research*, 98, 22987-22994.

Sausen, R., K. Barthel, and K. Hasselmann, 1988: Coupled ocean-atmosphere models with flux correction, *Climate Dynamics*, 2, 145-163.

Shackley, S., J. Risbey, P. Stone, and B. Wynne, 1999: Adjusting to policy expectations in climate change modeling: An interdisciplinary study of flux adjustments in coupled atmosphere-ocean general circulation models, *Climatic Change*, 43, 413-454.

Sokolov, A. and P.H. Stone, 1998: A flexible climate model for use in integrated assessments. *Climate Dynamics*, 14, 291 – 303.

Sokolov, A., C.E. Forest, and P.H. Stone, 2003: Comparing oceanic uptake in AOGCM transient climate change experiments, *Journal of Climate*, 16, 1573–1582.

Sokolov, A.P., C.A. Schlosser, S. Dutkiewicz, S. Paltsev, D.W. Kicklighter, H.D. Jacoby, R.G. Prinn, C.E. Forest, J. Reilly, C. Wang, B. Felzer, M.C. Sarofim, J. Scott, P.H. Stone, J.M. Melillo and J. Cohen, 2005: The MIT Integrated Global System Model (IGSM) Version 2: Model Description and Baseline Evaluation, *Joint Program on the Science and Policy of Global Change Report*, 124, MIT, Cambridge, MA.

Smith, S.J., R. Andres, E. Conception, and J. Lurz, 2004: Sulfur Dioxide Emissions: 1850-2000, *JGCRI Report* PNNL-14537.

Takahashi, T., S.C. Sutherland, C. Sweeney, A. Poisson, N. Metzl, B. Tilbrook, N. Bates, R. Wanninkhof, R.A. Feely, C. Sabine, J. Olafsson, and Y. Nojiri, 2002: Global sea-air CO_2 flux based on climatological surface ocean pCO_2, and seasonal biological and temperature effects, *Deep-Sea Research II*, 49, 1601 – 1622.

Trenberth, K., J. Olson, and W. Large, 1989: *A global wind stress climatology based on ECMWF analyses, Tech. Rep. NCAR/TN-338+STR*, National Center for Atmospheric Research, Boulder, Colorado.

Voss, R., R. Sausen, U. Cubasch, 1998: Periodically synchronouslly coupled integration with the atmosphere-ocean general circulation model ECHAM3/LSG, *Climate Dynamics*, 14, 249–266.

Wang, Y., and D. Jacob, 1998: Anthropogenic Forcing on Tropospheric Ozone and OH since Preindustrial Times, *Journal of Geophysical Research*, 103, 31123-31135.

Wang C. and R.G. Prinn, 1999: Impact of emissions, chemistry and climate on atmospheric carbon monoxide: 100-year predictions from a global chemistry-climate model. *Chemosphere-Global Change Science*, 1, 73–81.

Wang, C., R.G. Prinn, and A.P. Sokolov, 1998: A global interactive chemistry and climate model: Formulation and testing, *Journal of Geophysical Research*, 103, 3399–3417.

Wanninkhof, R., 1992: Relationship between wind speed and gas exchange over the ocean, *Journal of Geophysical Research*, 97, 7373 – 7382.

Webster, M.D., C.E. Forest, J.M. Reilly, M.H. Babiker, D. Kicklighter, M. Mayer, R. Prinn, M.C. Sarofim, A. Sokolov, P.H. Stone, and C. Wang, 2003: Uncertainty analysis of climate change and policy response. *Climatic Change*, 61, 295 – 320.

Wijffels, S.E., R.W. Schmitt, H. Bryden, and A. Stigebrand, 1992: Transport of freshwater by the ocean, *Journal of Physical Oceanography*, 22, 155–152.

Winton, M., 2000: A reformulated Three-layer Sea Ice Model. *Journal of Atmospheric and Ocean Technology*, 17, 525 – 531.

Yamanaka, Y. and E. Tajika, 1997: The role of dissolved organic matter in the marine biogeochemical cycle: Studies using and ocean biogeochemical general circulation model, *Global Biogeochemical Cycles*, 11, 599 – 612.

Yamanaka, Y. and E. Tajika, 1996: The role of the vertical fluxes of particulate organic matter and calcite in the oceanic carbon cycle: studies using an ocean biogeochemical circulation model, *Global Biogeochemical Cycles*, 10, 361 – 382.

Xiao, X., D.W. Kicklighter, J.M. Melillo, A.D. McGuire, P.H. Stone, and A.P. Sokolov, 1997: Linking a global terrestrial biogeochemical model and a 2-dimensional climate model: Implications for the carbon budget, *Tellus*, 49, 18–37.

Zeng, X., M. Shaikh, Y. Dai, R.E. Dickinson, and R. Myneni, 2002: Coupling of the Common Land Model to the NCAR Community Climate Model *Journal of Climate*, 15, 1832–1854.

Zhuang, Q., J.M. Melillo, D.W. Kicklighter, R.G. Prinn, A.D. McGuire, P.A. Steudler, B.S., Felzer, and S. Hu, 2004: Methane fluxes between terrestrial ecosystems and the atmosphere at the northern high latitudes during the past century: A retrospective analysis with a process-based biogeochemistry model, *Global Biogeochemical Cycles*, 18, GB3010, doi:10.1029/2004GB002239.

Zhuang, Q., A.D. McGuire, J.M. Melillo, J.S. Clein, R.J. Dargaville, D.W. Kicklighter, R.B. Myneni, J. Dong, V.E. Romanovsky, J. Harden and J.E. Hobbie, 2003: Carbon cycling in extratropical terrestrial ecosystems of the Northern Hemisphere during the 20th Century: A modeling analysis of the influences of soil thermal dynamics, *Tellus*, 55B: 751-776.

REPORT SERIES of the MIT *Joint Program on the Science and Policy of Global Change*

1. **Uncertainty in Climate Change Policy Analysis** *Jacoby & Prinn* Dec '94
2. **Description and Validation of the MIT Version of the GISS 2D Model** *Sokolov & Stone* June 1995
3. **Responses of Primary Production and Carbon Storage to Changes in Climate and Atmospheric CO_2 Concentration** *Xiao et al.* Oct 1995
4. **Application of the Probabilistic Collocation Method for an Uncertainty Analysis** *Webster et al.* Jan. 1996
5. **World Energy Consumption and CO_2 Emissions: 1950-2050** *Schmalensee et al.* April 1996
6. **The MIT Emission Prediction and Policy Analysis (EPPA) Model** *Yang et al.* May 1996
7. **Integrated Global System Model for Climate Policy Analysis** *Prinn et al.* June 1996 (*superseded by No. 36*)
8. **Relative Roles of Changes in CO_2 and Climate to Equilibrium Responses of Net Primary Production and Carbon Storage** *Xiao et al.* June 1996
9. **CO_2 Emissions Limits: *Economic Adjustments and the Distribution of Burdens*** *Jacoby et al.* July 1997
10. **Modeling the Emissions of N_2O & CH_4 from the Terrestrial Biosphere to the Atmosphere** *Liu* August 1996
11. **Global Warming Projections: *Sensitivity to Deep Ocean Mixing*** *Sokolov & Stone* September 1996
12. **Net Primary Production of Ecosystems in China and its Equilibrium Responses to Climate Changes** *Xiao et al.* Nov '96
13. **Greenhouse Policy Architectures and Institutions** *Schmalensee* November 1996
14. **What Does Stabilizing Greenhouse Gas Concentrations Mean?** *Jacoby et al.* November 1996
15. **Economic Assessment of CO_2 Capture and Disposal** *Eckaus et al.* December 1996
16. **What Drives Deforestation in the Brazilian Amazon?** *Pfaff* Dec 1996
17. **A Flexible Climate Model For Use In Integrated Assessments** *Sokolov & Stone* March 1997
18. **Transient Climate Change and Potential Croplands of the World in the 21st Century** *Xiao et al.* May 1997
19. **Joint Implementation: *Lessons from Title IV's Voluntary Compliance Programs*** *Atkeson* June 1997
20. **Parameterization of Urban Sub-grid Scale Processes in Global Atmospheric Chemistry Models** *Calbo et al.* July 1997
21. **Needed: A Realistic Strategy for Global Warming** *Jacoby, Prinn & Schmalensee* August 1997
22. **Same Science, Differing Policies; *The Saga of Global Climate Change*** *Skolnikoff* August 1997
23. **Uncertainty in the Oceanic Heat and Carbon Uptake & their Impact on Climate Projections** *Sokolov et al.* Sept 1997
24. **A Global Interactive Chemistry and Climate Model** *Wang, Prinn & Sokolov* September 1997
25. **Interactions Among Emissions, Atmospheric Chemistry and Climate Change** *Wang & Prinn* Sept. 1997
26. **Necessary Conditions for Stabilization Agreements** *Yang & Jacoby* October 1997
27. **Annex I Differentiation Proposals: *Implications for Welfare, Equity and Policy*** *Reiner & Jacoby* Oct. 1997
28. **Transient Climate Change and Net Ecosystem Production of the Terrestrial Biosphere** *Xiao et al.* November 1997
29. **Analysis of CO_2 Emissions from Fossil Fuel in Korea: 1961–1994** *Choi* November 1997
30. **Uncertainty in Future Carbon Emissions: *A Preliminary Exploration*** *Webster* November 1997
31. **Beyond Emissions Paths: *Rethinking the Climate Impacts of Emissions Protocols*** *Webster & Reiner* November 1997
32. **Kyoto's Unfinished Business** *Jacoby et al.* June 1998
33. **Economic Development and the Structure of the Demand for Commercial Energy** *Judson et al.* April 1998
34. **Combined Effects of Anthropogenic Emissions & Resultant Climatic Changes on Atmospheric OH** *Wang & Prinn* April 1998
35. **Impact of Emissions, Chemistry, and Climate on Atmospheric Carbon Monoxide** *Wang & Prinn* April 1998
36. **Integrated Global System Model for Climate Policy Assessment: *Feedbacks and Sensitivity Studies*** *Prinn et al.* June 98
37. **Quantifying the Uncertainty in Climate Predictions** *Webster & Sokolov* July 1998
38. **Sequential Climate Decisions Under Uncertainty: *An Integrated Framework*** *Valverde et al.* Sept. 1998
39. **Uncertainty in Atmospheric CO_2 (Ocean Carbon Cycle Model Analysis)** *Holian* Oct. 1998 (*superseded by No. 80*)
40. **Analysis of Post-Kyoto CO_2 Emissions Trading Using Marginal Abatement Curves** *Ellerman & Decaux* October 1998
41. **The Effects on Developing Countries of the Kyoto Protocol and CO_2 Emissions Trading** *Ellerman et al.* November 1998
42. **Obstacles to Global CO_2 Trading: *A Familiar Problem*** *Ellerman* Nov '98
43. **The Uses and Misuses of Technology Development as a Component of Climate Policy** *Jacoby* Nov. 1998
44. **Primary Aluminum Production: *Climate Policy, Emissions and Costs*** *Harnisch et al.* December 1998
45. **Multi-Gas Assessment of the Kyoto Protocol** *Reilly et al.* Jan '99
46. **From Science to Policy: *The Science-Related Politics of Climate Change Policy in the U.S.*** *Skolnikoff* January 1999
47. **Constraining Uncertainties in Climate Models Using Climate Change Detection Techniques** *Forest et al.* April 1999
48. **Adjusting to Policy Expectations in Climate Change Modeling** *Shackley et al.* May 1999
49. **Toward a Useful Architecture for Climate Change Negotiations** *Jacoby et al.* May 1999
50. **A Study of the Effects of Natural Fertility, Weather and Productive Inputs in Chinese Agriculture** *Eckaus & Tso* July '99
51. **Japanese Nuclear Power and the Kyoto Agreement** *Babiker, Reilly & Ellerman* August 1999
52. **Interactive Chemistry and Climate Models in Global Change Studies** *Wang & Prinn* September 1999
53. **Developing Country Effects of Kyoto-Type Emissions Restrictions** *Babiker & Jacoby* October 1999
54. **Model Estimates of the Mass Balance of the Greenland and Antarctic Ice Sheets** *Bugnion* October 1999
55. **Changes in Sea-Level Associated with Modifications of Ice Sheets over 21st Century** *Bugnion* Oct. 1999
56. **The Kyoto Protocol & Developing Countries** *Babiker et al.* Oct '99
57. **Can EPA Regulate Greenhouse Gases Before the Senate Ratifies the Kyoto Protocol?** *Bugnion & Reiner* November 1999
58. **Multiple Gas Control Under the Kyoto Agreement** *Reilly, Mayer & Harnisch* March 2000
59. **Supplementarity: *An Invitation for Monopsony?*** *Ellerman & Sue Wing* April 2000
60. **A Coupled Atmosphere-Ocean Model of Intermediate Complexity** *Kamenkovich et al.* May 2000
61. **Effects of Differentiating Climate Policy by Sector: *A U.S. Example*** *Babiker et al.* May 2000
62. **Constraining Climate Model Properties Using Optimal Fingerprint Detection Methods** *Forest et al.* May 2000
63. **Linking Local Air Pollution to Global Chemistry and Climate** *Mayer et al.* June 2000

Contact the Joint Program Office to request a copy. The Report Series is distributed at no charge.

REPORT SERIES of the MIT *Joint Program on the Science and Policy of Global Change*

64. **The Effects of Changing Consumption Patterns on the Costs of Emission Restrictions** *Lahiri et al.* Aug. 2000

65. **Rethinking the Kyoto Emissions Targets** *Babiker & Eckaus* Aug 2000

66. **Fair Trade and Harmonization of Climate Change Policies in Europe** *Viguier* September 2000

67. **The Curious Role of "Learning" in Climate Policy: *Should We Wait for More Data?*** *Webster* October 2000

68. **How to Think About Human Influence on Climate** *Forest et al.* Oct '00

69. **Tradable Permits for Greenhouse Gas Emissions: *A primer with reference to Europe*** *Ellerman* Nov. 2000

70. **Carbon Emissions and The Kyoto Commitment in the European Union** *Viguier et al.* February 2001

71. **The MIT Emissions Prediction and Policy Analysis Model: *Revisions, Sensitivities and Results*** *Babiker et al.* February 2001

72. **Cap and Trade Policies in the Presence of Monopoly and Distortionary Taxation** *Fullerton & Metcalf* March 2001

73. **Uncertainty Analysis of Global Climate Change Projections** *Webster et al.* March 2001 (*superseded by No. 95*)

74. **The Welfare Costs of Hybrid Carbon Policies in the European Union** *Babiker et al.* June 2001

75. **Feedbacks Affecting the Response of the Thermohaline Circulation to Increasing CO_2** *Kamenkovich et al.* July 2001

76. **CO_2 Abatement by Multi-fueled Electric Utilities: *An Analysis Based on Japanese Data*** *Ellerman & Tsukada* July 2001

77. **Comparing Greenhouse Gases** *Reilly et al.* July 2001

78. **Quantifying Uncertainties in Climate System Properties using Recent Climate Observations** *Forest et al.* July 2001

79. **Uncertainty in Emissions Projections for Climate Models** *Webster et al.* August 2001

80. **Uncertainty in Atmospheric CO_2 Predictions from a Global Ocean Carbon Cycle Model** *Holian et al.* September 2001

81. **A Comparison of the Behavior of AO GCMs in Transient Climate Change Experiments** *Sokolov et al.* Dec 2001

82. **The Evolution of a Climate Regime: *Kyoto to Marrakech*** *Babiker, Jacoby & Reiner* February 2002

83. **The "Safety Valve" and Climate Policy** *Jacoby & Ellerman* Feb 2002

84. **A Modeling Study on the Climate Impacts of Black Carbon Aerosols** *Wang* March 2002

85. **Tax Distortions & Global Climate Policy** *Babiker et al.* May '02

86. **Incentive-based Approaches for Mitigating GHG Emissions: *Issues and Prospects for India*** *Gupta* June 2002

87. **Deep-Ocean Heat Uptake in an Ocean GCM with Idealized Geometry** *Huang, Stone & Hill* September 2002

88. **The Deep-Ocean Heat Uptake in Transient Climate Change** *Huang et al.* September 2002

89. **Representing Energy Technologies in Top-down Economic Models using Bottom-up Info** *McFarland et al.* October 2002

90. **Ozone Effects on Net Primary Production and Carbon Sequestration in the U.S. Using a Biogeochemistry Model** *Felzer et al.* November 2002

91. **Exclusionary Manipulation of Carbon Permit Markets: *A Laboratory Test*** *Carlén* November 2002

92. **An Issue of Permanence: *Assessing the Effectiveness of Temporary Carbon Storage*** *Herzog et al.* Dec 2002

93. **Is International Emissions Trading Always Beneficial?** *Babiker et al.* December 2002

94. **Modeling Non-CO_2 Greenhouse Gas Abatement** *Hyman et al.* Dec '02

95. **Uncertainty Analysis of Climate Change and Policy Response** *Webster et al.* December 2002

96. **Market Power in International Carbon Emissions Trading: *A Laboratory Test*** *Carlén* January 2003

97. **Emissions Trading to Reduce Greenhouse Gas Emissions in the U.S.: *The McCain-Lieberman Proposal*** *Paltsev et al.* June '03

98. **Russia's Role in the Kyoto Protocol** *Bernard et al.* June 2003

99. **Thermohaline Circulation Stability: *A Box Model Study*** *Lucarini & Stone* June 2003

100. **Absolute vs. Intensity-Based Emissions Caps** *Ellerman & Sue Wing* July 2003

101. **Technology Detail in a Multi-Sector CGE Model: *Transport Under Climate Policy*** *Schafer & Jacoby* July 2003

102. **Induced Technical Change and the Cost of Climate Policy** *Sue Wing* September 2003

103. **Past and Future Effects of Ozone on Net Primary Production and Carbon Sequestration Using a Global Biogeochemical Model** *Felzer et al.* (revised) January 2004

104. **A Modeling Analysis of Methane Exchanges Between Alaskan Ecosystems & the Atmosphere** *Zhuang et al.* Nov 2003

105. **Analysis of Strategies of Companies under Carbon Constraint** *Hashimoto* January 2004

106. **Climate Prediction: *The Limits of Ocean Models*** *Stone* Feb '04

107. **Informing Climate Policy Given Incommensurable Benefits Estimates** *Jacoby* February 2004

108. **Methane Fluxes Between Ecosystems & Atmosphere at High Latitudes During the Past Century** *Zhuang et al.* March 2004

109. **Sensitivity of Climate to Diapycnal Diffusivity in the Ocean** *Dalan et al.* May 2004

110. **Stabilization and Global Climate Policy** *Sarofim et al.* July '04

111. **Technology and Technical Change in the MIT EPPA Model** *Jacoby et al.* July 2004

112. **The Cost of Kyoto Protocol Targets: *The Case of Japan*** *Paltsev et al.* July 2004

113. **Economic Benefits of Air Pollution Regulation in the USA: *An Integrated Approach*** *Yang et al.* (revised) Jan 2005

114. **The Role of Non-CO_2 Greenhouse Gases in Climate Policy: *Analysis Using the MIT IGSM*** *Reilly et al.* Aug 2004

115. **Future United States Energy Security Concerns** *Deutch* Sep '04

116. **Explaining Long-Run Changes in the Energy Intensity of the U.S. Economy** *Sue Wing* September 2004

117. **Modeling the Transport Sector: The Role of Existing Fuel Taxes in Climate Policy** *Paltsev et al.* Nov. 2004

118. **Effects of Air Pollution Control on Climate** *Prinn et al.* Jan '05

119. **Does Model Sensitivity to Changes in CO_2 Provide a Measure of Sensitivity to the Forcing of Different Nature?** *Sokolov* March 2005

120. **What Should the Government Do To Encourage Technical Change in the Energy Sector?** *Deutch* May 2005

121. **Climate Change Taxes and Energy Efficiency in Japan** *Kasahara et al.* May 2005

122. **A 3D Ocean-Seaice-Carbon Cycle Model and its Coupling to a 2D Atmospheric Model: *Uses in Climate Change Studies*** *Dutkiewicz et al.* May (revised November) 2005

123. **Simulating the Spatial Distribution of Population and Emissions to2100** *Asadoorian* May 2005

124. **MIT Integrated Global System Model (IGSM) Version2: *Model Description and Baseline Evaluation*** *Sokolov et al.* July 2005

125. **The MIT Emissions Prediction and Policy Analysis (EPPA) Model: Version4** *Paltsev et al.* August 2005

126. **Estimated PDFs of Climate System Properties Including Natural and Anthropogenic Forcings** *Forestet al.* September 2005

127. **An Analysis of the European Emission Trading Scheme** *Reilly & Paltsev* October 2005

128. **Evaluating the Use of Ocean Models of Different Complexity in Climate Change Studies** *Sokolov et al* November 2005

Contact the Joint Program Office to request a copy. The Report Series is distributed at no charge.